

Technical Report 09-08

**Physico-Chemical Characterisation
Data and Sorption Measurements
of Cs, Ni, Eu, Th, U, Cl, I and Se on
MX-80 Bentonite**

December 2011

M.H. Bradbury, B. Baeyens

Paul Scherrer Institut, Villigen PSI

**National Cooperative
for the Disposal of
Radioactive Waste**

Hardstrasse 73
CH-5430 Wettingen
Switzerland
Tel. +41 56 437 11 11

www.nagra.ch

Technical Report 09-08

**Physico-Chemical Characterisation
Data and Sorption Measurements
of Cs, Ni, Eu, Th, U, Cl, I and Se on
MX-80 Bentonite**

December 2011

M.H. Bradbury, B. Baeyens

Paul Scherrer Institut, Villigen PSI

**National Cooperative
for the Disposal of
Radioactive Waste**

Hardstrasse 73
CH-5430 Wettingen
Switzerland
Tel. +41 56 437 11 11

www.nagra.ch

This report was prepared on behalf of Nagra. The viewpoints presented and conclusions reached are those of the author(s) and do not necessarily represent those of Nagra.

ISSN 1015-2636

"Copyright © 2011 by Nagra, Wettingen (Switzerland) / All rights reserved.

All parts of this work are protected by copyright. Any utilisation outwith the remit of the copyright law is unlawful and liable to prosecution. This applies in particular to translations, storage and processing in electronic systems and programs, microfilms, reproductions, etc."

Preface

The Laboratory for Waste Management of the Nuclear Energy and Safety Research Department at the Paul Scherrer Institut is performing work to develop and test models as well as to acquire specific data relevant to performance assessments of Swiss radioactive waste repositories. These investigations are undertaken in close co-operation with, and with the financial support of, the National Cooperative for the Disposal of Radioactive Waste (Nagra). The present report is issued simultaneously as a PSI Bericht and a Nagra Technical Report.

Abstract

This report describes the work carried out in LES on MX-80 bentonite in support of Swiss radioactive waste performance assessment studies. With particular regard to Stage 2 of the Sectoral Plan for deep geological disposal, it was considered to be important to bring together in one document the information and results that have accrued over the years from both “in house” studies and associated relevant literature data. The report gives a brief overview of the physico-chemical characteristics and porewater chemistry determined for MX-80 bentonite followed by the results of an extensive experimental sorption programme on the uptake of Cs(I), Ni(II), Eu(III), Th(IV), U(VI), Cl(-I), I(-I) and Se(IV) on the same material. Sorption values are also given for K(I), Ca(II) and Sr(II) which were deduced from porewater chemistry modelling studies.

Zusammenfassung

In diesem Bericht werden die Arbeiten beschrieben, die am Labor für Endlagersicherheit zur Unterstützung der Sicherheitsanalysen für die Tiefenlagerung radioaktiver Abfälle in der Schweiz an MX-80 Bentonit durchgeführt wurden. Besonders in Hinblick auf Etappe 2 des Sachplanes geologische Tiefenlager wurde es als wichtig erachtet, die Informationen und Ergebnisse sowohl aus eigenen Studien als auch aus der relevanten Literatur in einem Dokument zusammenzustellen. Der Bericht gibt einen kurzen Überblick der physikochemischen Eigenschaften und der Porenwasserchemie des Bentonit MX-80. Es folgen die Ergebnisse eines umfangreichen experimentellen Sorptionsprogrammes zur Aufnahme von Cs(I), Ni(II), Eu(III), Th(IV), U(VI), Cl(-I), I(-I) und Se(IV) auf dieses Material. Auch für K(I), Ca(II) und Sr(II) werden Sorptionswerte angegeben, die aus der Modellierung der Porenwasserchemie abgeleitet wurden.

Résumé

Le présent rapport décrit les travaux qui ont été réalisés au LES sur la bentonite MX-80 dans le cadre des analyses de sûreté préalables à la réalisation de dépôts en profondeur pour les déchets radioactifs en Suisse. Il a semblé important, notamment dans la perspective de l'étape 2 du Plan sectoriel pour les dépôts en couches géologiques profondes, de présenter sous forme synthétique l'ensemble des informations et résultats accumulés au cours des années, qu'ils soient issus d'études internes ou de publications extérieures. Le rapport donne un bref aperçu des caractéristiques physico-chimiques et de la chimie de l'eau interstitielle déterminés pour la bentonite MX-80. Il présente ensuite les résultats d'un vaste programme d'expérimentation sur la sorption de Cs(I), Ni(II), Eu(III), Th(IV), U(VI), Cl(-I), I(-I) et Se(IV) sur ce matériau. Pour K(I), Ca(II) et Sr(II) figurent également des valeurs de sorption déduites des études de modélisation concernant la chimie de l'eau interstitielle.

Table of Contents

Abstract	II
Zusammenfassung.....	III
Résumé	IV
List of Tables.....	VII
List of Figures	IX
1 Introduction	1
2 Preamble.....	3
3 Mineralogy and physico-chemical characteristics of MX-80.....	5
3.1 Mineralogy.....	5
3.2 Chemical composition of MX-80	7
3.3 Cation exchange	9
3.3.1 Exchangeable cations.....	9
3.3.2 Cation occupancies on MX-80	9
3.3.3 Selectivity coefficients.....	10
3.4 Amphoteric surface edge sites	11
4 Porewater chemistry.....	13
4.1 Porewater composition	13
4.2 Conditioning of MX-80 bentonite	14
4.3 Trace element concentrations in synthetic (SBPW) and equilibrated (EBPW) bentonite porewaters	15
5 Experimental procedures for sorption experiments.....	17
5.1 Electrode calibration.....	17
5.2 Standard solutions.....	18
5.3 Radionuclides/assay.....	18
5.4 Stability tests.....	18
5.5 Wall sorption	19
5.6 Sorption kinetics	19
5.7 Isotherm measurements	20
5.8 Uncertainties	20
6 Results.....	21
6.1 K(I), Ca(II) and Sr(II) sorption data	21
6.2 Cs(I) sorption data	22
6.2.1 Cs kinetics.....	22
6.2.2 Cs isotherm	23
6.3 Ni(II) sorption data	24
6.3.1 Ni kinetics.....	24
6.3.2 Ni isotherm	25
6.4 Eu(III) sorption data	26

6.4.1	Eu kinetics	26
6.4.2	Eu isotherm	27
6.5	Th(IV) sorption data	28
6.5.1	Th kinetics	28
6.5.2	Th isotherm	29
6.6	U(VI) sorption data	30
6.6.1	U kinetics	30
6.6.2	U isotherm	31
6.7	Se(IV) sorption data	32
6.7.1	Se kinetics	32
6.7.2	Se isotherm	33
6.8	Cl(-I) and I(-I) sorption measurements	34
6.9	I(-I) sorption data	35
6.9.1	I(-I) kinetics at 153 g L ⁻¹	35
6.9.2	I(-I) kinetics at 303 g L ⁻¹	36
7	Summary	37
	Acknowledgements	39
	References	41

List of Tables

Table 3.2:	Iron content, and Cl ⁻ and SO ₄ inventories.....	6
Table 3.3:	Lattice density and surface areas of MX-80.....	6
Table 3.5:	Whole rock element analyses (mol kg ⁻¹) of 2 samples on “as received” and conditioned MX-80 bentonite.....	8
Table 3.6:	Summary of the cation occupancies and fraction occupancies on MX-80 bentonite.....	9
Table 3.7:	Selectivity coefficients for K-Na, Mg-Na and Ca-Na exchange equilibria on MX-80 corrected to zero ionic strength (I = 0).....	11
Table 3.8:	Summary of site types, site capacities, and protolysis constants for conditioned Na-montmorillonite. ($\equiv S^{W1}OH$, $\equiv S^{W2}OH$ denote the two weak site types which can protonate and de-protonate in the model of Bradbury & Baeyens 1997).	12
Table 4.1:	Calculated MX-80 bentonite porewater (BPW). The BPW is saturated with calcite, dolomite, gypsum, celestite, fluorite and quartz.	13
Table 4.2:	Synthetic and equilibrated bentonite porewater compositions used in the sorption isotherm measurements for Cs(I), Ni(II), Eu(III), Th(IV), U(VI), I(-I) and Se(IV) on MX-80. The ICP-OES analyses of each solution was done in duplicate and the mean values from 14 measurements together with the standard deviation (in brackets) are given.	14
Table 4.3:	Trace element analyses of SBPW and the EBPW analysed by ICP-MS (EMPA).	15
Table 5.1:	Highest stable starting concentrations of Cs, Ni, Eu, Th, U, I and Se used in the isotherm sorption measurements in the equilibrated bentonite porewater at pH = 7.6.	19
Table 6.1:	Sorption data for K, Ca and Sr on MX-80.....	21
Table 6.2:	Summary of the conditions used in the kinetic measurements of Cs on MX-80 bentonite in the porewater composition given in Table 4.2.....	22
Table 6.3:	Summary of the conditions used in the isotherm measurements of Cs on MX-80 bentonite.....	23
Table 6.4:	Summary of the conditions used in the kinetic measurements of Ni on MX-80 bentonite.....	24
Table 6.5:	Summary of the conditions used in the isotherm measurements of Ni on MX-80 bentonite.....	25
Table 6.6:	Summary of the conditions used in the kinetic measurements of Eu on MX-80 bentonite.....	26
Table 6.7:	Summary of the conditions used in the isotherm measurements of Eu on MX-80 bentonite.....	27
Table 6.8:	Summary of the conditions used in the kinetic measurements of Th on MX-80 bentonite.....	28

Table 6.9: Summary of the conditions used in the isotherm measurements of Th on MX-80 bentonite.....	29
Table 6.10: Summary of the conditions used in the kinetic measurements of U on MX-80 bentonite in the porewater composition given in Table 4.2.....	30
Table 6.11: Summary of the conditions used in the isotherm measurements of U on MX-80 bentonite.....	31
Table 6.12: Summary of the conditions used in the kinetic measurements of Se on MX-80 bentonite in the porewater composition given in Table 4.2.....	32
Table 6.13: Summary of the conditions used in the isotherm measurements of Se on MX-80 bentonite.....	33
Table 6.14: Calculated “ R_d values” and exclusion volumes for Cl ⁻	34
Table 6.15: Summary of the conditions used in the kinetic measurements of I on MX-80 bentonite.....	35
Table 6.16: Summary of the conditions used in the kinetic measurements of I on MX-80 bentonite.....	36

List of Figures

Fig. 2.1:	Sketch of the structure of montmorillonite (After Tsipursky & Drits 1984).....	3
Fig. 5.1:	Plot of the measured pH (pH_r) against known proton concentrations in 0.6 M NaCl.	17
Fig. 6.1:	Sorption kinetics of Cs uptake on MX-80 in batch experiments in the porewater composition given in Table 4.2.....	22
Fig. 6.2:	Sorption isotherm of Cs on MX-80 measured in batch experiments in the porewater composition given in Table 4.2. (From Table 4.3 the background concentration of Cs in the EBPW is 1.2×10^{-8} M, indicated by the dashed line.).....	23
Fig. 6.3:	Sorption kinetics of Ni uptake on MX-80 in batch experiments in the porewater composition given in Table 4.2.....	24
Fig. 6.4:	Sorption isotherm of Ni on MX-80 measured in batch experiments in the porewater composition given in Table 4.2. (From Table 4.3 the background concentration of Ni in the EBPW is $< 1.7 \times 10^{-8}$ M.).....	25
Fig. 6.5:	Sorption kinetics of Eu uptake on MX-80 in batch experiments in the porewater composition given in Table 4.2.....	26
Fig. 6.6:	Sorption isotherm of Eu on MX-80 measured in batch experiments in the porewater composition given in Table 4.2. (From Table 4.3 the background concentration of Eu in the EBPW is $< 3.3 \times 10^{-9}$ M.).....	27
Fig. 6.7:	Sorption kinetics of Th uptake on MX-80 in batch experiments in the porewater composition given in Table 4.2.....	28
Fig. 6.8:	Sorption isotherm of Th on MX-80 measured in batch experiments in the porewater composition given in Table 4.2. (From Table 4.3 the background concentration of Th in the EBPW is $< 4.3 \times 10^{-10}$ M.).....	29
Fig. 6.9:	Sorption kinetics of U uptake on MX-80 in batch experiments in the porewater composition given in Table 4.2.....	30
Fig. 6.10:	Sorption isotherm of U on MX-80 measured in batch experiments in the porewater composition given in Table 4.2. (From Table 4.3 the background concentration of U in the EBPW is 2.1×10^{-8} M, indicated by the dashed line.).....	31
Fig. 6.11:	Sorption kinetics of Se uptake on MX-80 in batch experiments.	32
Fig. 6.12:	Sorption isotherm of Se on MX-80 measured in batch experiments in the porewater composition given in Table 4.2. (From Table 4.3 the background concentration of Se in the EBPW is $< 1.3 \times 10^{-7}$ M.).....	33
Fig. 6.13:	Sorption kinetics of I uptake on MX-80 in batch experiments at 153 g L^{-1} in the porewater composition given in Table 4.2.....	35
Fig. 6.14:	Sorption kinetics of I uptake on MX-80 in batch experiments at 303 g L^{-1} in the porewater composition given in Table 4.2.....	36

1 Introduction

Bentonite, in one form or another (e.g. dry compacted blocks, compacted granules or in sand/bentonite mixtures) is foreseen as back-fill and sealing material in Swiss projects for deep geological repositories. The high swelling capacity of compacted bentonite upon re-saturation, its very low transmissivity to water movement and good sorption characteristics all contribute to making compacted bentonite an extremely effective near-field diffusion barrier to the movement of radionuclides.

This report is broadly divided into two main parts. The first part gives a brief overview of the physico-chemical characteristics and porewater chemistry determined for MX-80 bentonite followed by the results of extensive experimental sorption programme on the uptake of Cs(I), Ni(II), Eu(III), Th(IV), U(VI), Cl(-I), I(-I) and Se(IV) on the same material. These nuclides are representative for alkaline, transition metals, trivalent lanthanides/actinides, and tetravalent and hexavalent actinides respectively. Se and I were chosen because they are important dose determining nuclides in performance assessment. Sorption values are also given for K(I), Ca(II) and Sr(II) which were deduced from porewater chemistry modelling studies. The sorption of radionuclides on the immobile solids in the near-field back-fill and sealing materials is an important mechanism retarding the transport of radionuclides through these barriers.

The majority of the experiments reported here were carried out pre 2000 and have not previously been reported in detail. One of the main aims of the work is to provide documentation of the experimental data which has already been used, or will be used in the future, to develop sorption data bases for bentonite systems for performance assessment studies for radioactive waste repositories in Switzerland.

2 Preamble

Bentonites contain large quantities of montmorillonite (65 to 90 wt.%) and consequently their properties are largely determined by this clay mineral (see for example Grauer 1986).

The generally accepted structure of montmorillonite is a unit made of an alumina octahedral sheet sandwiched between two silica tetrahedral sheets, Fig. 2.1. The tetrahedral-octahedral-tetrahedral (TOT) layers have dimensions in the a and b directions of the order of 1000 nm and combine together, one above the another, in the c direction to form platelets. The thickness of these platelets are only a few individual montmorillonite layers. Larger clay particles are formed from stacks of these platelets (Grim 1953) in which the number of platelets in each stack varies from 3-5 in Na-montmorillonite to 10-20 (and more) for a Ca-montmorillonite (Pusch et al. 1990).

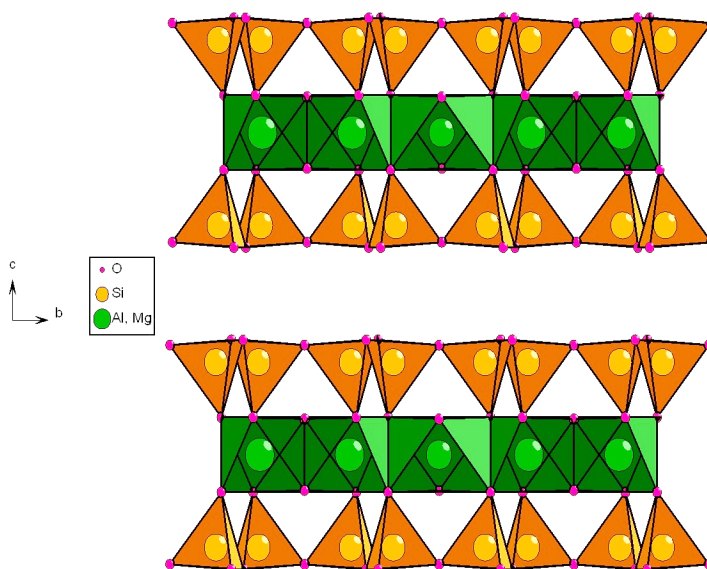


Fig. 2.1: Sketch of the structure of montmorillonite (After Tsipursky & Drits 1984).

Water and other polar molecules can enter between the unit layers causing expansion in the c direction (interlayer swelling). The c-axis lattice parameter is ~ 0.96 nm in the absence of any polar molecules in the interlayer. The interlayers in montmorillonite tend to take up water "layer-wise" and each monolayer of water increases the c-spacing by ~ 0.25 nm (Keren & Shainberg 1975; Newman 1987). In bentonite there are between 1 and 4 monolayers of H₂O in the interlayer space after re-saturation, depending on the initial dry density.

The total surface area of montmorillonites is very large, $\sim 7.5 \times 10^5$ m² kg⁻¹, and most of this area lies in the interlayer region. For comparison, the external specific surface area for Na- and Ca-montmorillonites are in the range of 1.5 to 9×10^4 m² kg⁻¹. (Grim 1953, Van Olphen & Fripiat 1979).

Substitution of trivalent Al for tetravalent Si in the tetrahedra and divalent cations (e.g. Mg, Fe) for trivalent Al in the octahedra of the montmorillonite structure leads to a permanent negative lattice charge which is compensated by the preferential sorption of cations on the layer surfaces. In aqueous systems these cations can exchange with those in solution, see section 3.3.

In addition to the cation exchange sites, another site type exists on the edges of the montmorillonite structural units. These "edge" sites are amphoteric, see section 3.4, and the properties of both site types play an important role in determining the sorption characteristics of bentonite.

In highly compacted bentonite there are large masses of montmorillonite and only small volumes of porewater (see Bradbury & Baeyens 2002) and hence the ion capacities of the solids are massively greater than those in the aqueous phase. The consequence of this is that montmorillonite and the other solid phases, through the cation loadings on the clay and solubility considerations respectively, will determine the composition of the porewater. In addition, the high exchange capacity of the montmorillonite component acts as a powerful buffer for the composition of the porewater (Bradbury & Baeyens 2002, 2009)

3 Mineralogy and physico-chemical characteristics of MX-80

3.1 Mineralogy

The MX-80 Na-Bentonite (Wyoming, USA) was obtained from Bentonit International GmbH, Duisburg (Germany). Samples of the "as received" powdered MX-80 were heated to constant weight in an oven at 105 °C. The water content was determined to be 7.1 wt.%.

Müller-Vonmoos & Kahr (1982, 1983) have characterized the MX-80 bentonite and have carried out a mineralogical analysis which is reproduced in Table 3.1. In this analysis ~2 wt.% of the material remained as "unidentified".

The average mineralogy of six samples of MX-80 from different consignments from 1980 to 2001 used in the Swedish SKB programme (Karnland, 2010) is also given in Table 3.1.

Table 3.1: Mineralogical composition of MX-80 bentonite. The compositions are expressed in wt.% of oven-dried MX-80.

Minerals	Müller-Vonmoos & Kahr (1982)	Karnland (2010)
Montmorillonite	75	81.4
Illite	-	0.8
Kaolinite	<1	-
Calcite	0.7	0.2
Cristobalite	-	0.9
Gypsum	-	0.9
Muscovite	-	3.4
K-feldspar	5-8	-
Plagioclase	-	3.5
Pyrite	0.3	0.6
Siderite	0.7	-
Quartz	15.2	3.0
Tridymite	-	3.8

The main point to note from Table 3.1 is that the montmorillonite content is by far the dominant mineral in MX-80. The differences in the results for the accessory minerals are probably due to the different XRD evaluation tools used for the analyses.

Total and amorphous iron(hydr)oxide, chloride and sulphate inventories are given in Table 3.2.

Table 3.2: Iron content, and Cl⁻ and SO₄ inventories.

Other constituents	(mmol kg⁻¹)	References
amorphous iron	10.6 ± 0.4	Bradbury & Baeyens (2002)
total iron	25.9 ± 0.7	
NaCl	1.35 ± 0.1	Bradbury & Baeyens (2002)
	1.04 ± 0.2	Wanner et al. (1992)
CaSO ₄	23.5 ± 0.9	Bradbury & Baeyens (2002)
	26.6 ± 4.2	Wanner et al. (1992)

Some additional relevant characteristics of MX-80 are summarised in Table 3.3 for completeness.

Table 3.3: Lattice density and surface areas of MX-80.

Physical property	Data values	Source reference
Lattice density (kg m ⁻³)	2755	Müller-Vonmoos & Kahr (1983)
N ₂ BET specific surface area (m ² g ⁻¹)	30	Kruse (1992)
	31.3	Bradbury & Baeyens (1998a)
Ethylene glycol total surface area (m ² g ⁻¹)	562	Müller-Vonmoos & Kahr (1983)

3.2 Chemical composition of MX-80

MX-80 bentonite samples were analysed at the Service d'Analyses des Roches et des Minéraux (SARM), in Nancy, France. The crushed rock samples were fused with LiBO_2 and dissolved in HNO_3 and then analysed for major and trace elements by ICP-OES and ICP-MS respectively. Two samples each of "as received" MX-80 and conditioned MX-80 (see section 4.2) were analysed and the results for major and minor elements of each sample are given in Tables 3.4 and 3.5 respectively. The uncertainties in the rock analyses depend on the concentration levels and are generally below 5 %. At concentrations close to the detection limits the uncertainty increase to ~ 20 %.

The results of major element analyses for the SKB reference MX-80 bentonite (Karnland 2010) are also given in Table 3.4, and the correspondence between the analyses is very good.

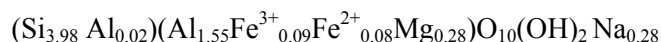
Table 3.4: The chemical composition of MX-80 expressed as weight percent of major element oxides after ignition.

	SiO ₂	Al ₂ O ₃	Fe ₂ O ₃	MgO	CaO	Na ₂ O	K ₂ O	TiO ₂	P ₂ O ₅
As received MX-80									
Sample A	66.84	20.48	5.06	2.49	1.45	2.65	0.53	0.20	0.10
Sample B	66.90	20.47	5.04	2.47	1.44	2.61	0.53	0.19	0.12
Conditioned MX-80									
Sample A	66.84	20.50	4.93	2.66	1.45	2.62	0.50	0.20	0.10
Sample B	66.71	20.60	4.94	2.66	1.44	2.62	0.49	0.20	0.10
MX-80 from SKB[#]									
MX-80 mean	67.4	21.2	4.14	2.61	1.46	2.25	0.55	0.17	0.05
STDEV	1.13	0.45	0.20	0.13	0.14	0.26	0.04	0.03	0.01

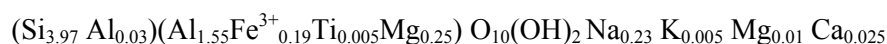
[#]Taken from Karnland (2010). „MX-80 mean“ is the average chemical composition of 6 bentonite samples taken from different consignments representing more than 20 years of production.

Structural formula of the montmorillonite in MX-80

The structural formula of the montmorillonite fraction of MX-80 bentonite was investigated by Sauzéat et al. (2001) and yielded the following unit cell formula for the Na-saturated form:



For comparison, the structural formula of montmorillonite in the SKB reference MX-80 was given by Karnland (2010) as:



The correspondence between both formulae is good, but there are some differences e.g. Fe^{3+} content.

Table 3.5: Whole rock element analyses (mol kg⁻¹) of 2 samples on “as received” and conditioned MX-80 bentonite.

Element	“As received” MX-80		Conditioned MX-80	
	Sample A	Sample B	Sample A	Sample B
As	1.6 E-04	1.6 E-04	1.3 E-04	1.3 E-04
Ba	2.9 E-03	2.8 E-03	2.5 E-03	2.5 E-03
Be	2.1 E-04	1.9 E-04	1.9 E-04	2.2 E-04
Bi	3.9 E-06	3.7 E-06	4.1 E-06	4.6 E-06
Cd	3.7 E-06	4.3 E-06	2.8 E-06	< 2.7 E-06
Ce	7.2 E-04	6.8 E-04	7.1 E-04	7.0 E-04
Co	4.0 E-05	3.6 E-05	3.8 E-05	3.6 E-05
Cr	2.0 E-04	1.0 E-04	1.0 E-04	< 9.6 E-05
Cs	8.3 E-06	6.4 E-06	4.5 E-06	9.5 E-06
Cu	1.3 E-04	1.1 E-04	9.5 E-05	1.3 E-04
Dy	4.0 E-05	3.8 E-05	3.9 E-05	4.0 E-05
Er	2.1 E-05	1.9 E-05	1.9 E-05	2.0 E-05
Eu	5.1 E-06	5.0 E-06	4.7 E-06	4.7 E-06
Ga	4.0 E-04	4.0 E-04	3.8 E-04	3.9 E-04
Gd	5.3 E-05	4.6 E-05	4.9 E-05	4.8 E-05
Ge	1.3 E-05	1.0 E-05	1.1 E-05	1.1 E-05
Hf	4.0 E-05	4.0 E-05	3.8 E-05	3.9 E-05
Ho	7.9 E-06	7.6 E-06	7.7 E-06	7.7 E-06
In	< 8.7 E-07	< 8.7 E-07	< 8.7 E-07	< 8.7 E-07
La	3.5 E-04	3.4 E-04	3.4 E-04	3.4 E-04
Lu	2.8 E-06	2.7 E-06	2.6 E-06	2.7 E-06
Mo	3.4 E-05	3.3 E-05	1.4 E-05	1.4 E-05
Nb	2.9 E-04	2.8 E-04	2.8 E-04	2.7 E-04
Nd	3.0 E-04	3.0 E-04	2.9 E-04	3.0 E-04
Ni	1.3 E-04	1.2 E-04	1.3 E-04	1.3 E-04
Pb	1.9 E-04	2.0 E-04	1.8 E-04	2.0 E-04
Pr	8.5 E-05	8.2 E-05	8.2 E-05	8.2 E-05
Rb	1.6 E-04	1.4 E-04	1.2 E-04	1.3 E-04
Sb	1.1 E-05	1.1 E-05	9.5 E-06	9.4 E-06
Se	1.9 E-06	2.0 E-06	1.1 E-06	1.1 E-06
Sm	6.3 E-05	6.3 E-05	6.3 E-05	6.3 E-05
Sn	6.8 E-05	6.2 E-05	6.5 E-05	6.4 E-05
Sr	2.7 E-03	2.7 E-03	2.0 E-03	1.9 E-03
Ta	1.6 E-05	1.5 E-05	1.6 E-05	1.7 E-05
Tb	7.7 E-06	7.3 E-06	7.6 E-06	7.3 E-06
Th	1.6 E-04	1.5 E-04	1.5 E-04	1.7 E-04
Tm	3.1 E-06	3.0 E-06	3.1 E-06	3.2 E-06
U	5.2 E-05	4.7 E-05	4.6 E-05	5.0 E-05
V	2.8 E-04	2.6 E-04	2.6 E-04	2.6 E-04
W	2.0 E-06	2.0 E-06	2.1 E-06	2.3 E-06
Y	4.0 E-04	3.9 E-04	3.9 E-04	3.8 E-04
Yb	1.9 E-05	1.8 E-05	1.9 E-05	1.9 E-05
Zn	1.9 E-03	2.0 E-03	1.2 E-03	1.3 E-03
Zr	2.2 E-03	2.1 E-03	2.0 E-03	1.9 E-03

3.3 Cation exchange

3.3.1 Exchangeable cations

The surfaces of montmorillonite clay platelets carry a permanent negative charge arising from isomorphous substitution of lattice cations by cations of a lower valency. Charge neutrality is maintained by the presence of an excess of cations in solution held electrostatically in close proximity around the outside of the Si-Al-Si clay units. Since the areas within the interlayer space are predominant, the compensating cations reside mainly there. The electrostatically bound cations, which constitute the electrical double layer, can undergo stoichiometric exchange with the cations in solution (Grim 1953, Van Olphen 1963). The total permanent negative charge of a clay mineral is defined as the cation exchange capacity (CEC). The exchange capacities of montmorillonites are high, $\sim 1 \text{ Eq. kg}^{-1}$, and since the MX-80 bentonite contains $\sim 75 \text{ wt.}\%$ montmorillonite, this implies that its exchange capacity is also significant.

3.3.2 Cation occupancies on MX-80

The cation occupancies and equivalent fraction occupancies (N_B values) were deduced for the "as received" MX-80 bentonite powder in a series of Ni-ethylenediamine extraction tests (Maes & Cremers 1986, Peigneur 1976, Bradbury & Baeyens 2002). The equivalent fraction occupancies are defined as:

$$N_B = \frac{\text{Quantity of cation B on the permanent charge sites of the clay minerals (meq kg}^{-1}\text{)}}{\text{CEC (meq kg}^{-1}\text{)}} \quad (3.1)$$

where $B = \text{Na}^+, \text{K}^+, \text{Mg}^{2+}, \text{Ca}^{2+}$ or Sr^{2+} .

The results are summarised in Table 3.6.

Table 3.6: Summary of the cation occupancies and fraction occupancies on MX-80 bentonite.

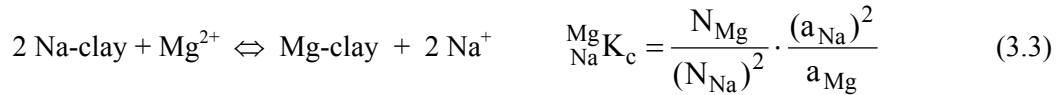
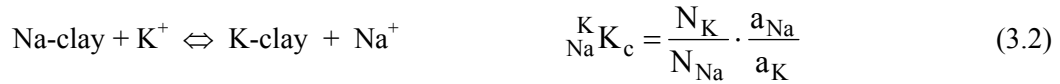
Cation	Cation occupancy (meq kg ⁻¹)	Fractional occupancy (N_B values)
Na	668 ± 40	0.85 ± 0.05
K	13 ± 2	0.017 ± 0.003
Mg	40 ± 3	0.051 ± 0.004
Ca	66 ± 3	0.084 ± 0.004
Sr [#]		
Σ Cations	787 ± 48	

[#] The Sr occupancy is calculated (see section 6.1)

The cation exchange capacity is taken to be the sum of the individual occupancies and yields a value of $787 \pm 48 \text{ meq kg}^{-1}$. This value is in good agreement with the CEC data from Müller-Vonmoos & Kahr (1983) on MX-80 bentonite. These authors obtained CEC values between $767 - 780 \text{ meq kg}^{-1}$ using the ammonium acetate method ($\text{pH} = 7$). The cation occupancies for Na, Mg and K given in Müller-Vonmoos & Kahr (1983) are generally lower than the data given in Table 6, i.e. 624 meq kg^{-1} for Na, 30 meq kg^{-1} for Mg and 2 meq kg^{-1} for K. The datum for Ca is slightly higher i.e. 74 meq kg^{-1} . The CEC measurements obtained on five different consignments of MX-80 using the Cu-trien method yielded values between $710 - 770 \text{ meq kg}^{-1}$ (Karnland 2010).

3.3.3 Selectivity coefficients

Selectivity coefficients, K_c , for K, Mg, and Ca have been calculated with respect to Na for the MX-80 system. Na was chosen as the reference cation since it is the most abundant cation present. The exchange reactions, and the associated mass action equations defining the selectivity coefficients according to the Gaines & Thomas (1953) convention, are given below:



where "a" represents solution activities and N_{Na} , N_{K} , N_{Mg} and N_{Ca} are equivalent fractional cation occupancies.

The fractional cation occupancies given in Table 3.6 were used together with the concentrations of Na, K, Mg, and Ca measured in aqueous extraction experiments, expressed in terms of cation activities, to calculate selectivity coefficients from Eqs. (3.2) to (3.4). The values for K-Na, Mg-Na and Ca-Na are summarised in Table 3.7. (See Bradbury & Baeyens (2002) for details of the methodology.)

From the mass action relations (Eqns. 3.2 to 3.4) it can be readily appreciated that the uncertainty in K_c depends upon the errors in the respective fractional occupancies, N_B values, and the aqueous concentrations. The error estimates given in Table 3.6 were used for the former and an error of $\pm 10\%$ for the latter. The maximum uncertainties in selectivity coefficients calculated on this basis are included with the K_c values in Table 3.7. Note that the selectivity coefficient for Mg-Na exchange was calculated from the Ca-Na value determined here over a literature value for Ca-Mg exchange (Bruggenwert & Kamphorst 1982, Sposito & Fletcher 1985). The fractional uncertainty in the Mg-Na values was taken to be the same as that for the Ca-Na selectivities.

Table 3.7: Selectivity coefficients for K-Na, Mg-Na and Ca-Na exchange equilibria on MX-80 corrected to zero ionic strength ($I = 0$).

Selectivity coefficients ($I = 0$)	S:L ratio (18.6 g L ⁻¹)	S:L ratio (27.9 g L ⁻¹)	S:L ratio (37.2 g L ⁻¹)	Mean values
$\frac{K}{Na}K_c$	4.6 ± 1.9	3.9 ± 1.6	3.6 ± 1.5	4.0 ± 1.6
$\frac{Mg}{Na}K_c$	2.2 ± 1.1	2.0 ± 1.0	2.3 ± 1.2	2.2 ± 1.1
$\frac{Ca}{Na}K_c$	2.6 ± 1.2	2.4 ± 1.1	2.7 ± 1.3	2.6 ± 1.2

Note: The selectivity coefficient of Sr with respect to Na was taken to be the same as the Ca-Na value because the occupancy of Sr on the as received MX-80 was too low to measure reliably in the Ni-en extraction experiments (Bradbury & Baeyens 2002).

The calculated selectivity coefficients for the different S:L ratios are not significantly different from one another and are compatible with literature values, $\frac{K}{Na}K_c = 2 - 5$; $\frac{Ca}{Na}K_c = 2 - 4$ (Bruggenwert & Kamphorst 1982, Sposito et al. 1983a,b).

3.4 Amphoteric surface edge sites

There is a second category of reactive sites associated with montmorillonite which are perceived as being surface hydroxyl groups ($\equiv\text{SOH}$) situated along the edges of the clay platelets, "edge" or "broken bond" sites. (See for example Bolt & Van Riemsdijk 1987) These sites have a capacity of ~ 10% of the CEC and can protonate and deprotonate so that the concentrations of neutral, protonated and deprotonated edge sites ($\equiv\text{SOH}$, $\equiv\text{SOH}_2^+$, $\equiv\text{SO}^-$ respectively) change as a function of pH. Using a similar argument to the one given above for the cation exchange sites, the hydroxyl groups can potentially function as a powerful pH buffer (Bradbury & Baeyens 2002, 2009).

For completeness, $\equiv\text{SOH}$ site types, capacities and protolysis constants for montmorillonite are given in Table 3.8. These values were obtained from the analyses of batch titration experiments (Baeyens & Bradbury 1997, Bradbury & Baeyens 1997) i.e. on dispersed systems. In compacted bentonite the spacings between the edges of clay stacks may become very small resulting in the overlap of electrical double layers. The implications of this for the protolysis behaviour of the $\equiv\text{SOH}$ edge sites is not clear, but could influence their amphoteric characteristics.

Table 3.8: Summary of site types, site capacities, and protolysis constants for conditioned Namontmorillonite. ($\equiv S^{W1}OH$, $\equiv S^{W2}OH$ denote the two weak site types which can protonate and de-protonate in the model of Bradbury & Baeyens 1997).

Site types:	Site capacities:	
$\equiv S^{W1}OH$	$4.0 \times 10^{-2} \text{ mol kg}^{-1}$	
$\equiv S^{W2}OH$	$4.0 \times 10^{-2} \text{ mol kg}^{-1}$	
Surface complexation reaction	Mass action equation	log K_{int}
$\equiv S^{W1}OH + H^+ \Leftrightarrow \equiv S^{W1}OH_2^+$	$K_{\text{int}}(+)=\frac{[\equiv S^{W1}OH_2^+]}{[\equiv S^{W1}OH] \cdot \{H^+\}}$	4.5
$\equiv S^{W1}OH \Leftrightarrow \equiv S^{W1}O^- + H^+$	$K_{\text{int}}(-)=\frac{[\equiv S^{W1}O^-] \cdot \{H^+\}}{[\equiv S^{W1}OH]}$	-7.9
$\equiv S^{W2}OH + H^+ \Leftrightarrow \equiv S^{W2}OH_2^+$	$K_{\text{int}}(+)=\frac{[\equiv S^{W2}OH_2^+]}{[\equiv S^{W2}OH] \cdot \{H^+\}}$	6.0
$\equiv S^{W2}OH \Leftrightarrow \equiv S^{W2}O^- + H^+$	$K_{\text{int}}(-)=\frac{[\equiv S^{W2}O^-] \cdot \{H^+\}}{[\equiv S^{W2}OH]}$	-10.5

Note: [] are concentrations; { } are activities

4 Porewater chemistry

4.1 Porewater composition

The majority of the sorption experiments reported here were carried out before the year 2000 as important inputs to the sorption data base for MX-80 required for the Entsorgungsnachweis (Nagra 2002). This was well before a conceptual model for calculating the porewater in compacted bentonite was fully developed, and also before the necessary data for such calculations were available. However, in order to carry out the sorption experiments, a bentonite porewater had to be defined. This was done on the basis of the incomplete information and knowledge available at the time (Bradbury & Baeyens unpublished results). The calculated porewater composition is given in Table 4.1.

Table 4.1: Calculated MX-80 bentonite porewater (BPW). The BPW is saturated with calcite, dolomite, gypsum, celestite, fluorite and quartz, and is in equilibrium with atmospheric $p\text{CO}_2$.

Parameter	BPW
Temperature	25 °C
pH	7.64
$p\text{CO}_2$	$10^{-3.5}$ bar
Ionic strength	0.7 M
Dissolved constituents	Concentration (M)
Na	5.68×10^{-1}
K	2.80×10^{-3}
Mg	2.31×10^{-2}
Ca	3.01×10^{-2}
Sr	2.66×10^{-4}
Al	4.16×10^{-8}
F	1.22×10^{-4}
Cl	6.19×10^{-1}
SO_4	2.92×10^{-2}
$\text{C}_{\text{inorg.}}$	4.23×10^{-4}
Si	1.81×10^{-4}

In the meantime, additional and improved information became available and some years later Bradbury & Baeyens (2002) published a porewater chemistry for bentonite where the pH was slightly higher (pH ~ 8) and the ionic strength lower ($I = 0.33$ M). Later, a reference MX-80 porewater for the Entsorgungsnachweis was defined in which a 20 times higher equilibrium partial pressure of CO_2 was assumed which resulted in an estimated pH of ~7.3 but the same ionic strength (Curti & Wersin 2002). Almost all of the information required for such porewater calculations comes from the publication of Bradbury & Baeyens (2002) e.g. saturated phases (calcite, gypsum, celestite, fluorite and quartz), chloride and sulphate inventories, cation occupancies, selectivity coefficients, amphoteric edge site capacities, protolysis constants etc.

All of the chemicals used were of the highest available purity grade and were purchased from Merck (Darmstadt, Germany) or Fluka (Buchs, Switzerland). Solutions were prepared with ultrapure deionised water obtained from a Milli-Q® Reagent Grade Water System purchased from Millipore (Molsheim, France).

4.2 Conditioning of MX-80 bentonite

Prior to each series of sorption measurements, MX-80 bentonite was conditioned to the synthetic bentonite porewater (SBPW). The aim of this procedure was to produce an MX-80 suspension which was in equilibrium with the major elements in the SBPW. The procedure was as follows. 20 g of MX-80 and 2 litres of synthetic MX-80 bentonite porewater were equilibrated in air and pH was adjusted to 7.6. After equilibration the clay was allowed to flocculate and the supernatant was separated from the clay. This solution, denoted as equilibrated bentonite porewater (EBPW), was subsequently centrifuged and used for the preparation of the solutions for the isotherm measurements. The exact clay content of the remaining MX-80 suspension was determined by heating 5 ml of the suspension overnight at 105 °C and weighing the residue. The dry weight of 20 ml EBPW was determined in the same manner in order to make salt corrections.

For each radionuclide isotherm determination on MX-80 a separate conditioning step was carried out, and in each case the SBPW and the EBPW was analysed by ICP-OES. The results are summarised in Table 4.2. The major ion concentrations in the SBPW and the EBPW after the conditioning process are essentially the same.

Table 4.2: Synthetic and equilibrated bentonite porewater compositions used in the sorption isotherm measurements for Cs(I), Ni(II), Eu(III), Th(IV), U(VI), I(-I) and Se(IV) on MX-80. The ICP-OES analyses of each solution was done in duplicate and the mean values from 14 measurements together with the standard deviation (in brackets) are given.

Dissolved constituents	SBPW (M)	EBPW (M)
Na	$5.65 \times 10^{-1} (9 \times 10^{-3})$	$5.65 \times 10^{-1} (9 \times 10^{-3})$
K	$2.82 \times 10^{-3} (6 \times 10^{-5})$	$2.80 \times 10^{-3} (4 \times 10^{-5})$
Mg	$2.23 \times 10^{-2} (6 \times 10^{-4})$	$2.22 \times 10^{-2} (4 \times 10^{-4})$
Ca	$2.99 \times 10^{-2} (3 \times 10^{-4})$	$3.00 \times 10^{-2} (3 \times 10^{-4})$
Sr*	$2.90 \times 10^{-4} (6 \times 10^{-6})$	$2.92 \times 10^{-4} (1 \times 10^{-5})$
SO ₄ *	$3.22 \times 10^{-2} (4 \times 10^{-4})$	$3.22 \times 10^{-2} (6 \times 10^{-4})$
Si	$1.24 \times 10^{-4} (4 \times 10^{-5})$	$1.44 \times 10^{-4} (4 \times 10^{-5})$
Al	$5.1 \times 10^{-6} (1.8 \times 10^{-6})$	$4.2 \times 10^{-6} (2.7 \times 10^{-6})$
Fe	$5.8 \times 10^{-7} (3.8 \times 10^{-7})$	$3.5 \times 10^{-7} (2.1 \times 10^{-7})$

* In the SBPW recipe the total Sr and SO₄ concentrations were set to 2.8×10^{-4} M and 3.0×10^{-2} M respectively. MOPS buffer (2.0×10^{-3} M) was present in the SBPW.

4.3 Trace element concentrations in synthetic (SBPW) and equilibrated (EBPW) bentonite porewaters

In the case of one series of experiments (section 4.2), trace element concentrations in the SBPW and in the equilibrated solution, EBPW, were analysed by high resolution ICP-MS at EMPA, Dübendorf, Switzerland. The uncertainties in the analyses are $\sim \pm 10\%$.

The results in Table 4.3 indicate that for most analysed elements the concentrations are below detection limits. However, an increase in background concentration in the EBPW is observed for Ba, Ce, Co, Cs, Fe, Ho, Mo, Rb, Sb and U.

The trace element concentrations given for the EBPW for the radionuclides investigated in this work (with the exception of iodine) represent the lowest concentrations at which sorption can be measured in the batch type tests carried out here.

Table 4.3: Trace element analyses of SBPW and the EBPW analysed by ICP-MS (EMPA).

Element	SBPW		EBPW	
	Sample A	Sample B	Sample A	Sample B
Ba	6.5 E-08	1.1 E-08	6.3 E-07	6.2 E-07
Bi	< 4.8 E-10		< 4.8 E-10	
Cd	< 8.9 E-10		< 8.9 E-10	
Ce	< 7.1 E-10		3.4 E-09	3.3 E-09
Co	< 1.7 E-09		9.7 E-09	9.8 E-09
Cr	< 1.9 E-08		< 1.9 E-08	
Cs	7.8 E-10	< 7.5 E-10	1.3 E-08	1.2 E-08
Cu	< 7.9 E-08		< 7.9 E-08	
Eu	< 3.3 E-09		< 3.3 E-09	
Fe	4.8 E-08	< 1.8 E-08	2.8 E-07	2.5 E-07
Hf	< 5.6 E-09		< 5.6 E-09	
Ho	< 6.1 E-10	8.6 E-10	1.1 E-09	1.3 E-09
Mo	2.5 E-09	2.2 E-09	2.1 E-07	2.2 E-07
Nb	< 1.1 E-08		< 1.1 E-08	
Nd	< 6.9 E-10		< 6.9 E-10	
Ni	< 1.7 E-08		< 1.7 E-08	
Pb	< 4.8 E-09		< 4.8 E-09	
Rb	< 1.2 E-08		1.9 E-07	2.0 E-07
Sb	2.6 E-09	2.2 E-09	8.7 E-09	9.1 E-09
Se	< 1.3 E-07		< 1.3 E-07	
Sn	< 8.4 E-09		< 8.4 E-09	
Th	< 4.3 E-10		< 4.3 E-10	
U	< 4.2 E-10		2.0 E-08	2.1 E-08
Zn	< 7.7 E-07		< 7.7 E-07	
Zr	< 1.1 E-08		< 1.1 E-08	

5 Experimental procedures for sorption experiments

In the following, general procedures used in the batch sorption experiments are described. Details specific to the individual experiments e.g. nuclide concentrations, S:L ratios, equilibration times and any deviation from the normal procedures are given in the appropriate sections.

5.1 Electrode calibration

Sorption experiments were carried out in ~0.6 M NaCl solutions. All pH measurements were carried out on a Metrohm 691 pH meter using Metrohm double junction pH electrode. The electrode was calibrated against known hydrogen ion concentrations at this NaCl background concentration. Solutions containing 10^{-1} , 10^{-2} and 10^{-3} M acid were made up using Merck Titrisol HCl analytical grade reagents in the presence of 0.6 M NaCl. As an illustration, a calibration curve of measured proton concentration (pH_r) against the minus logarithm of (fixed) proton concentrations is given for an ionic strength of 0.6 M in Fig. 5.1.

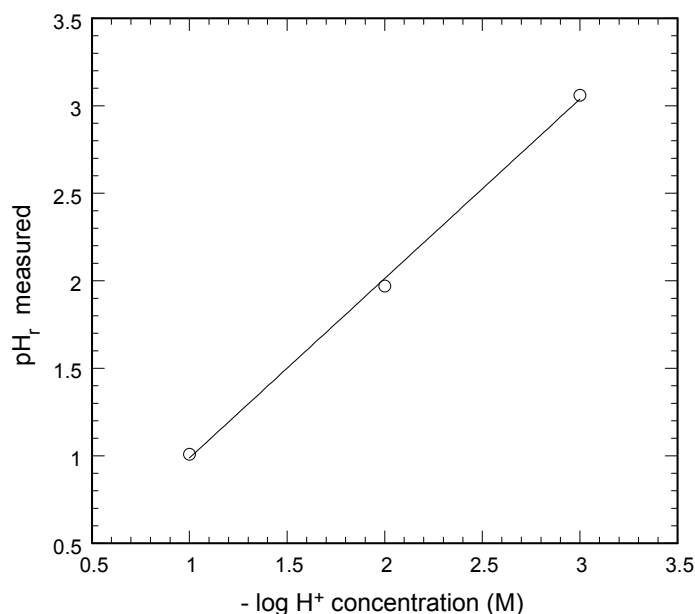


Fig. 5.1: Plot of the measured pH (pH_r) against known proton concentrations in 0.6 M NaCl.

Linear regression for the data yields:

$$pH_r = (-0.04 \pm 0.08) + (1.025 \pm 0.04) p[H^+] \quad (5.1)$$

In all further data evaluations the measured pH_r is taken to be the corresponding $p[H^+]$ value with an uncertainty of ± 0.1 log units.

The associated regression equation, which is electrode specific, was used to convert measured pH_r readings to proton activities (pH) using the following relation

$$\text{pH} = -\log \gamma_{\text{H}} + \text{pH}_r \quad (5.2)$$

where γ_{H} is the proton activity coefficient calculated using the Davies equation (Davies 1962),

$$\log \gamma_{\text{H}} = -0.511 z_i^2 \left(\frac{\sqrt{I}}{1 + \sqrt{I}} - 0.3 I \right) \quad (5.3)$$

where z_i is the charge and I the ionic strength.

This procedure was used throughout this work and applies to all pH values given.

5.2 Standard solutions

Sorption isotherms were measured in conditioned SBPW, Table 4.1. A solution of conditioned SBPW containing the highest stable concentration of the nuclide in question, see Table 5.1, were successively diluted with conditioned SBPW to yield a range of standard solutions containing different nuclide concentrations.

The standard solutions were labelled by adding known quantities of radioisotope. These labelled standard solutions were allowed to stabilise for at least one day in their polyethylene containers before use in the sorption tests in order to allow wall sorption to proceed to completion. A number of samples of these standard solutions (reference activities) were always counted simultaneously with the sample solutions from the batch sorption tests.

5.3 Radionuclides/assay

The radioisotopes ^{63}Ni , ^{134}Cs , ^{152}Eu and ^{75}Se were obtained from Amersham International Ltd. (Buckinghamshire, GB). ^{228}Th was purchased from Isotope Products Laboratories (California, USA). A 4.3×10^{-3} M solution of ^{233}U was available in house. An ICP-MS analysis (VG Elemental Plasma Quad 2) of this ^{233}U solution yielded the following isotopic composition: 99.94 % ^{233}U , 0.02 % ^{234}U and 0.04 % ^{238}U indicating that the purity of the ^{233}U solution was sufficient and could be used in the sorption experiments.

Radiochemical assays of ^{63}Ni and ^{233}U were carried out on a Canberra Packard TRI-CARB 2250CA or TRI-CARB 2750 TR/LL liquid scintillation analyzer. The radioisotopes ^{134}Cs , ^{152}Eu , ^{228}Th and ^{75}Se were radio assayed on a Canberra Packard Cobra Quantum gamma-counter.

5.4 Stability tests

Solubility calculations for Cs(I), Ni(II), Eu(III), Th(IV), U(VI) and Se(IV) in the synthetic MX-80 porewaters at pH = 7.6 were carried out using the geochemical code MINEQL (Westall et al. 1976) and the thermodynamic data base compilations (Pearson & Berner 1991, and Pearson et al. 1992), to estimate the experimental conditions for which each nuclide should be stable. Since the thermodynamic data cannot always be relied upon, the stabilities of the above nuclides were experimentally checked prior to performing the sorption experiments. The procedure was as follows: A series of salt solutions of the above nuclides at given concentrations were prepared in the synthetic MX-80 porewater and were kept for a time period of 3 days to one week. The solutions were then analysed by ICP-OES before and after centrifugation (1 hour at 96000 g max.) and if their concentrations remained constant it was concluded that they were stable.

Table 5.1 presents the highest (stable) starting concentrations used for each element for which isotherms were measured in the two different synthetic MX-80 porewaters.

Table 5.1: Highest stable starting concentrations of Cs, Ni, Eu, Th, U, I and Se used in the isotherm sorption measurements in the equilibrated bentonite porewater at pH = 7.6.

Element	EBPW (M)
Cs	3.3×10^{-3}
Ni	1.3×10^{-4}
Eu	1.9×10^{-6}
Th	4.0×10^{-7}
U	1.0×10^{-6}
Se	1.3×10^{-3}
I	1.0×10^{-3}

5.5 Wall sorption

Wall sorption is unavoidable in batch tests and their effects on sorption must be evaluated. The measuring of wall sorption in blank tests in the absence of the solid phase is not valid since competitive sorption effects between the solid phase and the wall are ignored.

In the studies of Ni and Zn sorption on Na-montmorillonite (Baeyens & Bradbury 1995) an acid leaching procedure was used on the test tubes after completion of the sorption experiments. These acid leaching tests showed that in the presence of Na-montmorillonite the extent of wall sorption was dependent on pH, the magnitude of sorption and on the S:L ratio. Generally the effects were very low and introduced a maximum uncertainty in the log R_d values of ~ 0.05 log units.

In a separate study Lauber et al. (2000) carried out wall sorption tests for the very strongly sorbing tracers Eu(III) and Th(IV) on Opalinus clay for which the sorption of these elements is similar to that on MX-80. Because of the low solubilities and high sorption, the tests were carried out at low S:L ratios (0.4 g L^{-1}). For each of the elements above the amount of radionuclide sorbed on the wall of the bottles was determined using the following procedure: 5 ml (Eu and Th) homogeneous aliquots of suspension were sampled from each bottle after a given time interval before centrifugation. The activity of these suspensions was then compared with the initial activity of the standard solutions (the activity measurements were solely carried out by gamma-counting). In all cases no differences between the initial activity and the activity in the suspensions after equilibration were measured indicating that even in the presence of small amounts of sorbent no significant wall sorption occurred.

5.6 Sorption kinetics

During the sorption isotherm experiments, sorption kinetic tests were performed with all of the radionuclides. (See the individual data sets for details). The procedure was to carry out kinetic tests at two or three of the concentrations chosen for the determination of the isotherm, trace and

one or two "high" concentrations. When the kinetic tests indicated that "equilibrium" (steady-state) conditions were reached, samples were taken at some convenient time after this at all of the concentrations.

5.7 Isotherm measurements

Sorption isotherms, i.e. the uptake of radionuclides as function of the radionuclide equilibrium concentration at constant pH in a conditioned SBPW (pH = 7.6) were performed for Cs(I), Ni(II), Eu(III), Th(IV), U(VI), I(-I) and Se(IV). The experiments were carried out under atmospheric conditions.

For Cs, Ni, Eu, Th, U (partly), I and Se the isotherm experiments were conducted at fixed solid to liquid (S:L) ratios and the total radionuclide concentration was varied. Depending on the expected sorption values the S:L ratio was chosen to be low (high R_d) or high (low R_d).

In the case of U additional experiments were carried out in which the highest total concentration was kept constant and the S:L ratio varied. Changing the S:L ratio allowed a series of measurements to be made near the maximum stable concentration level (Table 5.1) thus extending the isotherm measurement to the highest equilibrium concentrations possible without causing precipitation.

The general procedure for the isotherm measurements was as follows. Aliquots of MX-80 suspensions are added to a certain amount of appropriate labelled standard solution into 40 ml centrifuge tubes and shaken end-over-end for times up to 119 days. (Experiments were always performed in duplicate.) After the kinetic experiments indicated that equilibrium sorption had been attained, two samples at each concentration were centrifuged (1 hour at 95,000g max.) and two aliquots of the supernatant solutions were taken for radio assay together with the standard samples. The counting times were chosen to give ≤ 0.7 sigma errors. pH measurements were made in the remaining supernatant solution in each centrifuge tube.

5.8 Uncertainties

Estimates of the maximum error in each operation in similar batch sorption tests to those performed in this work have been done by Baeyens & Bradbury (1995) and yielded an uncertainty in $\log R_d$ of ~ 0.15 log units. When sorption experiments were repeated the R_d values varied within ± 0.2 log units. This uncertainty was taken to be realistic and all R_d values in this work are given with this error. This error estimate includes all possible sources of errors (e.g. weighing, volumetric and counting errors).

6 Results

The sorption results in this work are presented as distribution ratios R_d ($L\ kg^{-1}$) against time (kinetics) and equilibrium concentrations (isotherm). The distribution ratio R_d is defined as:

$$R_d = \frac{C_{init.} - C_{eq.}}{C_{eq.}} \cdot \frac{V}{m} \quad (6.1)$$

where,

$C_{init.}$: Total initial aqueous nuclide concentration (radioactive and stable) (M)

$C_{eq.}$: Total equilibrium aqueous nuclide concentration (radioactive and stable) (M)

V: volume of liquid phase (L)

m: mass of solid phase (kg)

The sorption isotherms are also presented as the quantity of nuclide sorbed ($mol\ kg^{-1}$) versus equilibrium concentration. In the cases of Cs and U their background concentration in the EBPW, Table 4.3, placed a limit on the lowest equilibrium concentration at which sorption could be measured.

6.1 K(I), Ca(II) and Sr(II) sorption data

Sorption data for the alkaline and alkaline-earth cations are derived directly from the bentonite porewater modelling, see section 3.3 and Table 4.1. Table 6.3 summarises the parameters required for the derivation of the R_d values.

The Sr-Na selectivity coefficient was assumed to be the same as the Ca-Na selectivity coefficient and the occupancy was calculated assuming saturation with respect to celestite ($SrSO_4$).

Table 6.1: Sorption data for K, Ca and Sr on MX-80.

Cation	Fractional occupancy (N_B)	Amount sorbed ($mmol\ kg^{-1}$)	Conc. in porewater (M)	R_d ($L\ kg^{-1}$)
K	0.017	13.4	2.80×10^{-3}	4.8
Ca	0.084	33.1	3.01×10^{-2}	1.1
Sr	0.0007	0.28	2.66×10^{-4}	1.1

CEC = 787 meq kg^{-1}

6.2 Cs(I) sorption data

6.2.1 Cs kinetics

Table 6.2: Summary of the conditions used in the kinetic measurements of Cs on MX-80 bentonite in the porewater composition given in Table 4.2.

Time (days)	S:L ratio (g L ⁻¹)	Total conc. (M)	pH
1; 7; 21; 39	60	3×10^{-3} ; 10^{-8}	7.6 - 7.7

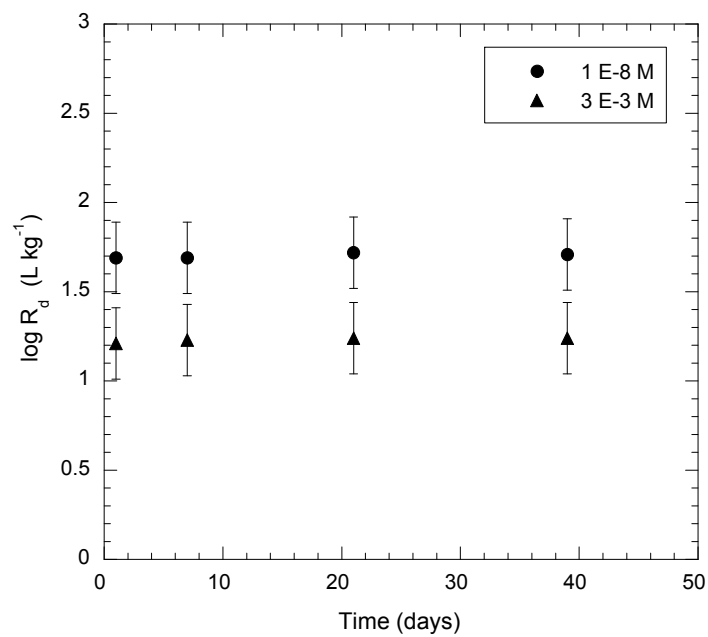


Fig. 6.1: Sorption kinetics of Cs uptake on MX-80 in batch experiments in the porewater composition given in Table 4.2.

6.2.2 Cs isotherm

Table 6.3: Summary of the conditions used in the isotherm measurements of Cs on MX-80 bentonite.

Time (days)	S:L ratio (g L ⁻¹)	Equilibrium conc. range (M)	pH
53	60	1.6 x 10 ⁻³ to 1.2 x 10 ⁻⁸	7.6 - 7.7

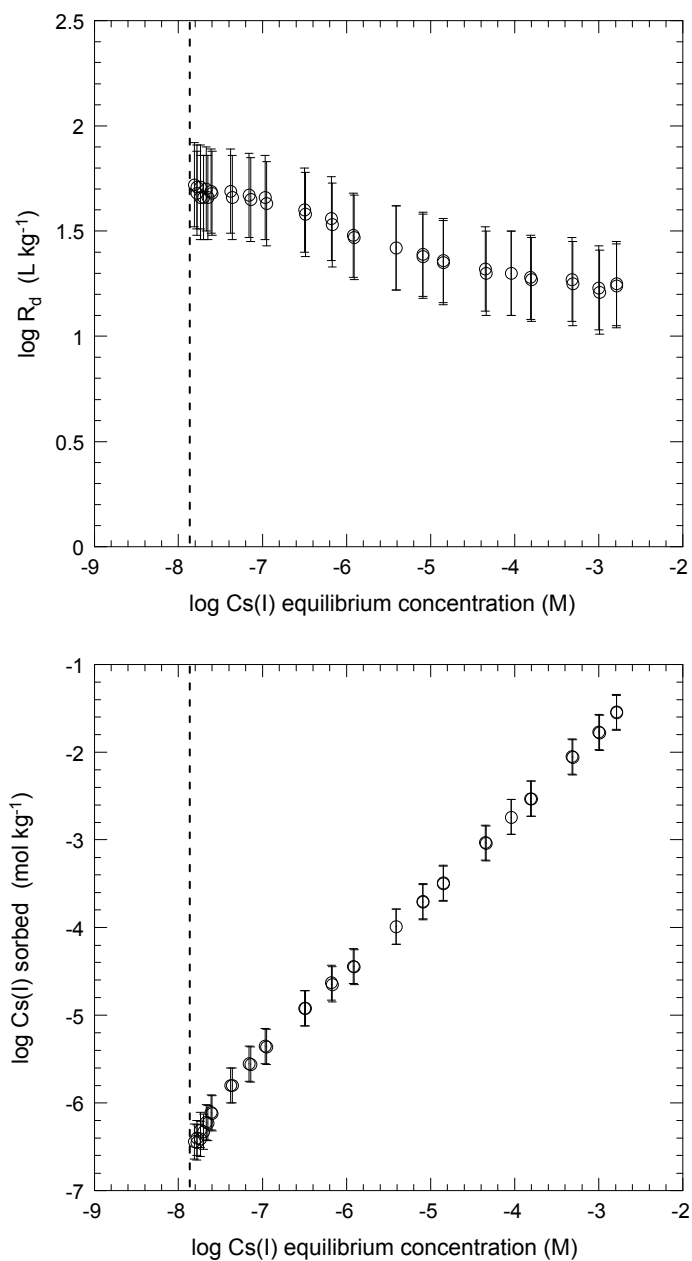


Fig. 6.2: Sorption isotherm of Cs on MX-80 measured in batch experiments in the porewater composition given in Table 4.2. (From Table 4.3 the background concentration of Cs in the EBPW is 1.2 x 10⁻⁸ M, indicated by the dashed line.)

6.3 Ni(II) sorption data

6.3.1 Ni kinetics

Table 6.4: Summary of the conditions used in the kinetic measurements of Ni on MX-80 bentonite.

Time (days)	S:L ratio (g L ⁻¹)	Total conc. (M)	pH
1; 7; 21; 61	1.56	1.2×10^{-4} ; 1.3×10^{-5} ; 7.1×10^{-9}	7.5 - 7.7

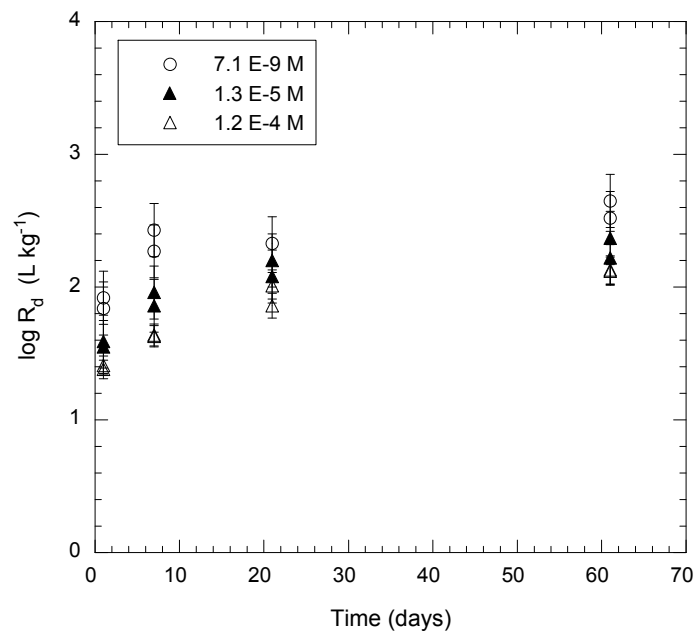


Fig. 6.3: Sorption kinetics of Ni uptake on MX-80 in batch experiments in the porewater composition given in Table 4.2

6.3.2 Ni isotherm

Table 6.5: Summary of the conditions used in the isotherm measurements of Ni on MX-80 bentonite.

Time (days)	S:L ratio (g L ⁻¹)	Equilibrium conc. range (M)	pH
74	1.56	1.0 x 10 ⁻⁴ to 5.6 x 10 ⁻⁹	7.4 - 7.6

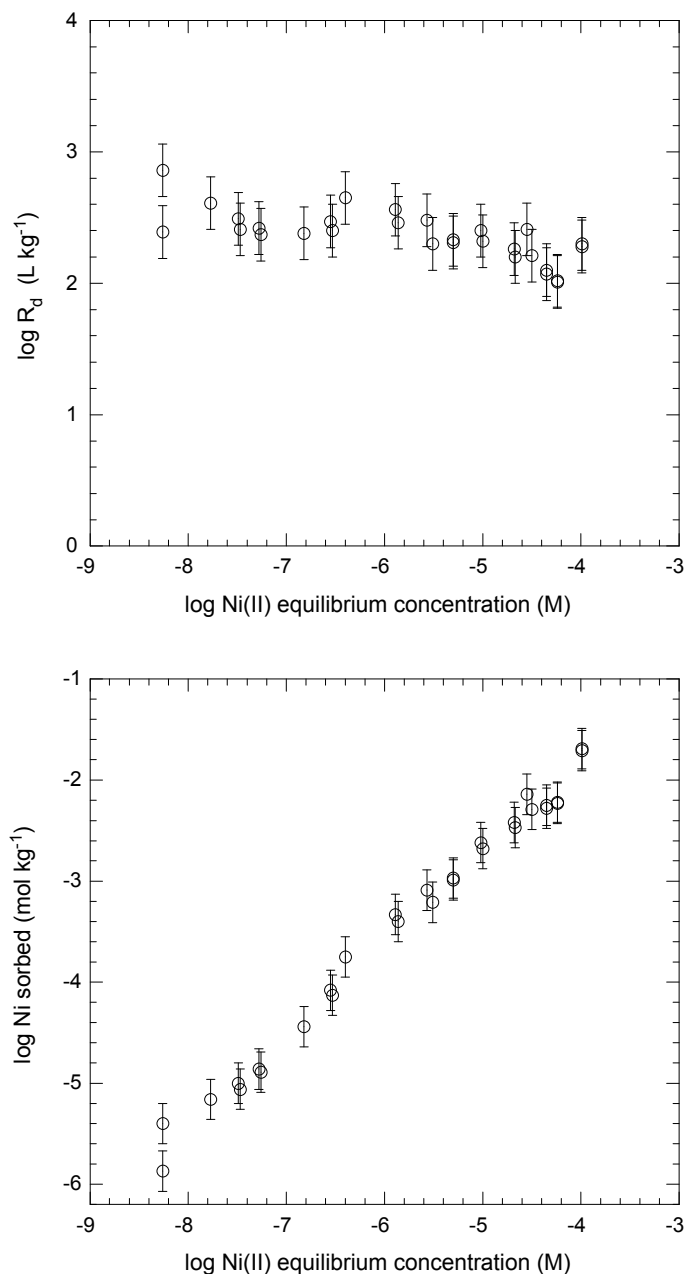


Fig. 6.4: Sorption isotherm of Ni on MX-80 measured in batch experiments in the porewater composition given in Table 4.2. (From Table 4.3 the background concentration of Ni in the EBPW is $< 1.7 \times 10^{-8}$ M.)

6.4 Eu(III) sorption data

6.4.1 Eu kinetics

Table 6.6: Summary of the conditions used in the kinetic measurements of Eu on MX-80 bentonite.

Time (days)	S:L ratio (g L ⁻¹)	Total conc. (M)	pH
1; 7; 21; 61	1.56	1.3×10^{-6} ; 3.3×10^{-7} ; 7.7×10^{-10}	7.5 - 7.6

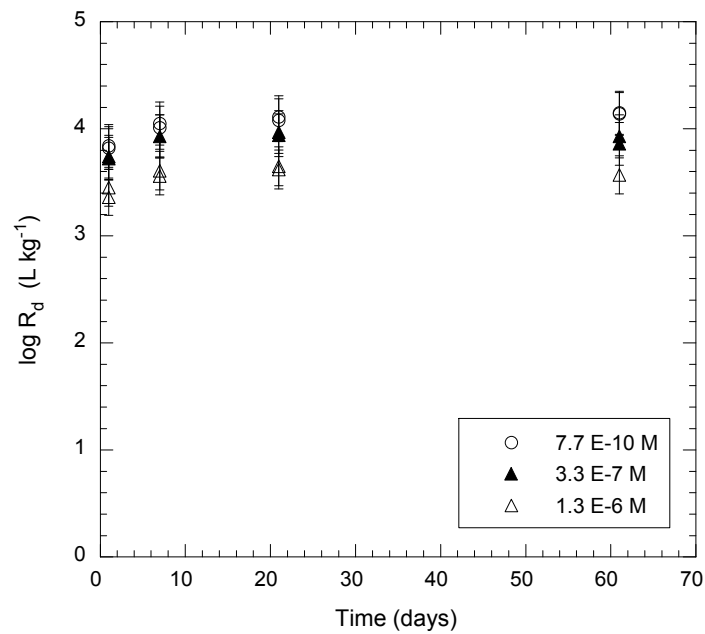


Fig. 6.5: Sorption kinetics of Eu uptake on MX-80 in batch experiments in the porewater composition given in Table 4.2.

6.4.2 Eu isotherm

Table 6.7: Summary of the conditions used in the isotherm measurements of Eu on MX-80 bentonite.

Time (days)	S:L ratio (g L ⁻¹)	Equilibrium conc. range (M)	pH
69	1.56	1.6 x 10 ⁻⁶ to 3.2 x 10 ⁻¹¹	7.4 - 7.6

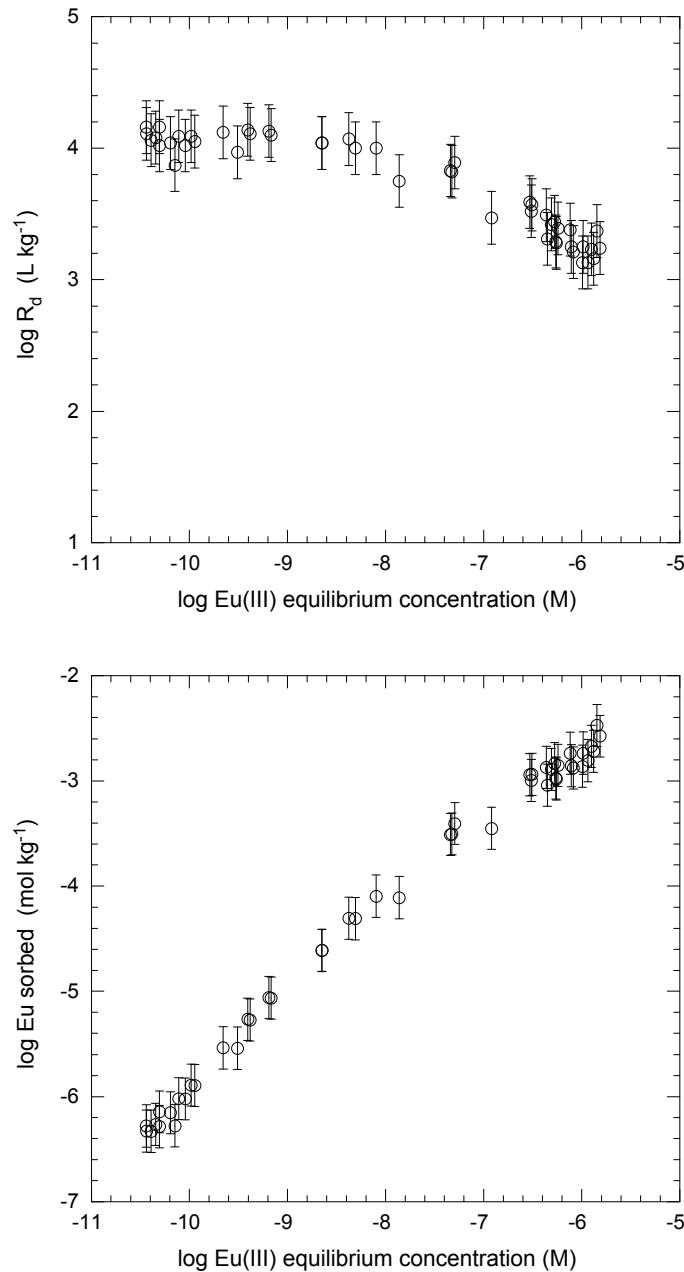


Fig. 6.6: Sorption isotherm of Eu on MX-80 measured in batch experiments in the porewater composition given in Table 4.2. (From Table 4.3 the background concentration of Eu in the EBPW is $< 3.3 \times 10^{-9}$ M.)

6.5 Th(IV) sorption data

6.5.1 Th kinetics

Table 6.8: Summary of the conditions used in the kinetic measurements of Th on MX-80 bentonite.

Time (days)	S:L ratio (g L ⁻¹)	Total conc. (M)	pH
1; 7; 21; 61	1.56	4 x 10 ⁻⁷ ; 4 x 10 ⁻⁸ ; 4 x 10 ⁻¹¹	7.1 - 7.8

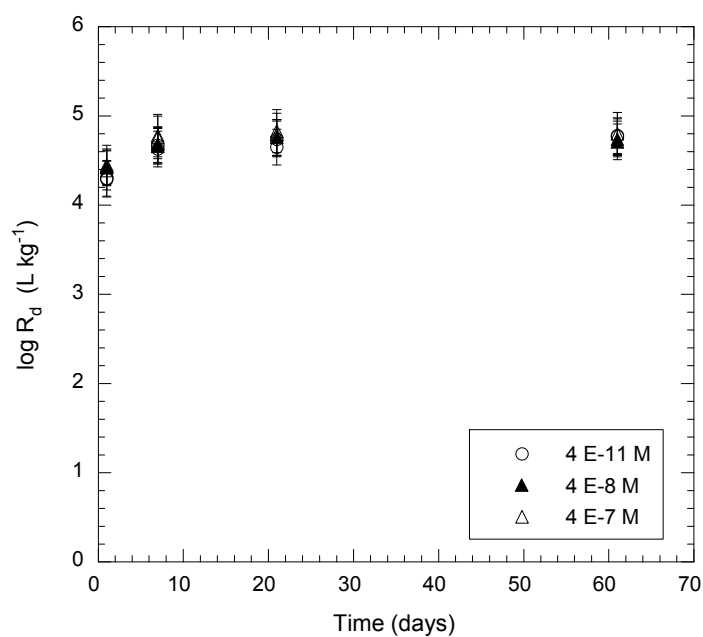


Fig. 6.7: Sorption kinetics of Th uptake on MX-80 in batch experiments in the porewater composition given in Table 4.2.

6.5.2 Th isotherm

Table 6.9: Summary of the conditions used in the isotherm measurements of Th on MX-80 bentonite.

Time (days)	S:L ratio (g L ⁻¹)	Equilibrium conc. range (M)	pH
119	1.56	5.0 x 10 ⁻⁹ to 5.0 x 10 ⁻¹³	7.1 - 7.6

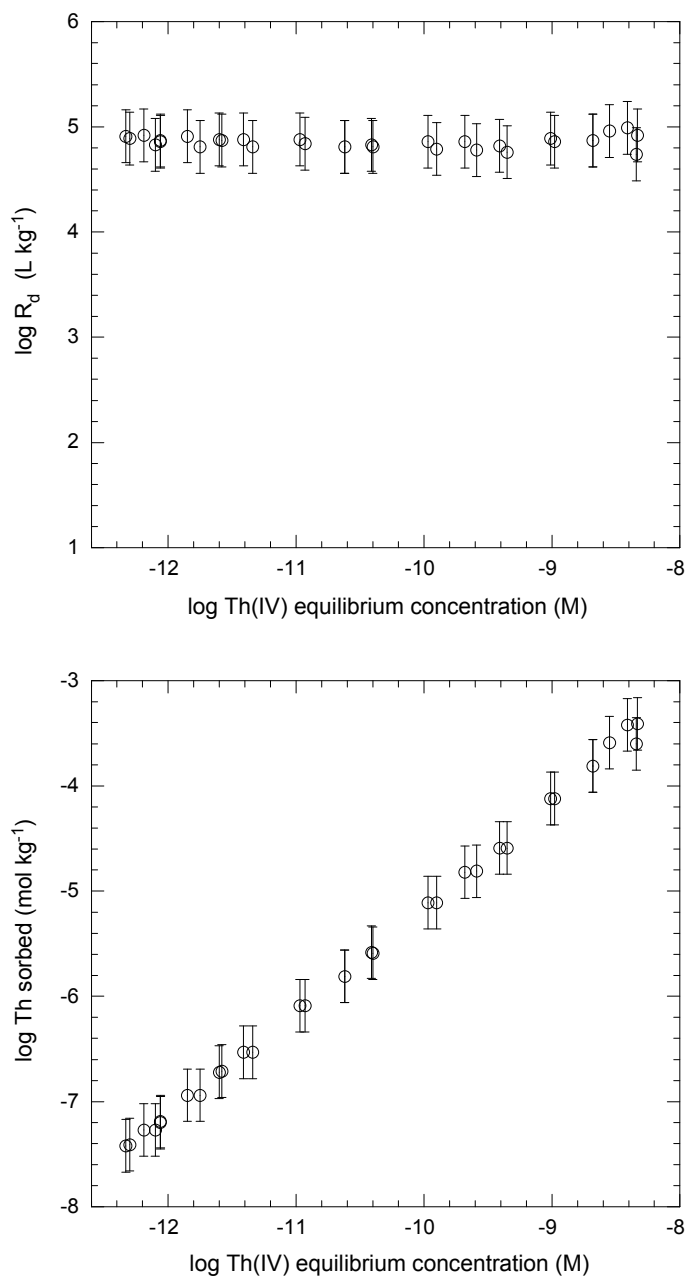


Fig. 6.8: Sorption isotherm of Th on MX-80 measured in batch experiments in the porewater composition given in Table 4.2. (From Table 4.3 the background concentration of Th in the EBPW is $< 4.3 \times 10^{-10}$ M.)

6.6 U(VI) sorption data

6.6.1 U kinetics

Table 6.10: Summary of the conditions used in the kinetic measurements of U on MX-80 bentonite in the porewater composition given in Table 4.2.

Time (days)	S:L ratio (g L ⁻¹)	Total conc. (M)	pH
8; 21; 35; 56	0.3 and 13.2	10 ⁻⁶ ; 3 x 10 ⁻⁸	7.6

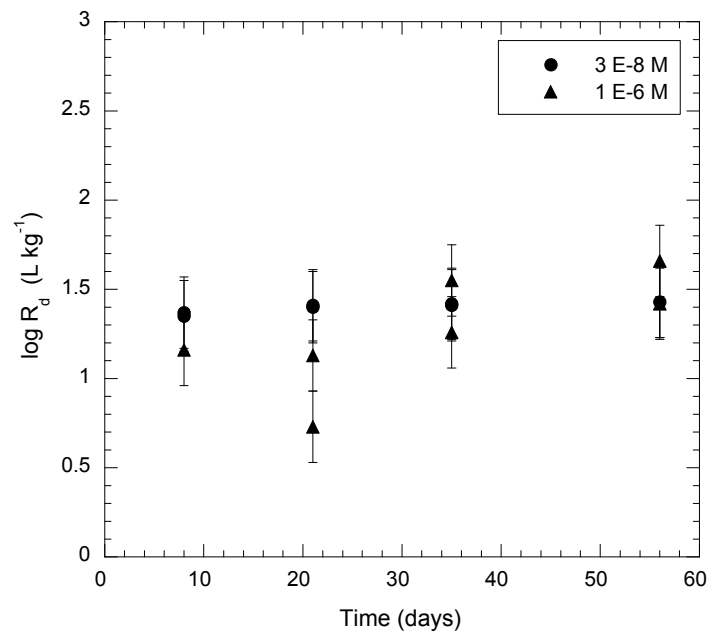


Fig. 6.9: Sorption kinetics of U uptake on MX-80 in batch experiments in the porewater composition given in Table 4.2.

6.6.2 U isotherm

Table 6.11: Summary of the conditions used in the isotherm measurements of U on MX-80 bentonite.

Time (days)	S:L ratio (g L ⁻¹)	Equilibrium conc. range (M)	pH
70	0.32 - 13.5	1.0 x 10 ⁻⁶ to 3.0 x 10 ⁻⁸	7.6

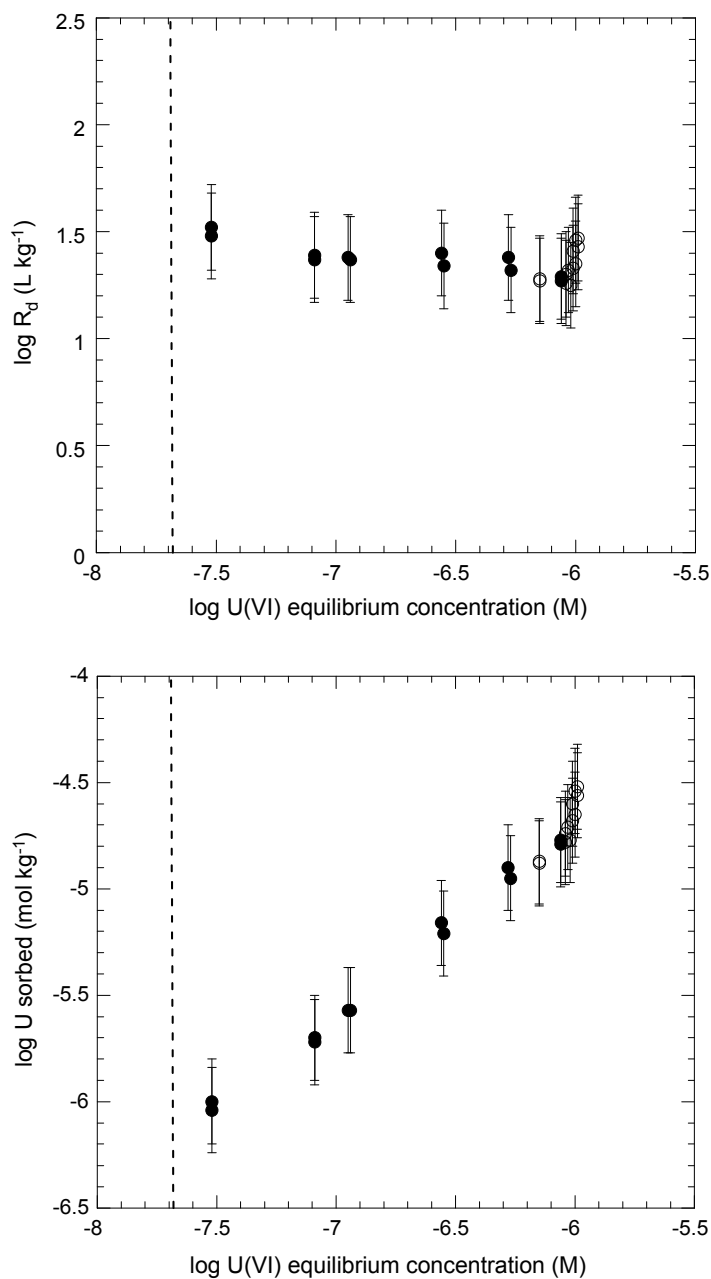


Fig. 6.10: Sorption isotherm of U on MX-80 measured in batch experiments in the porewater composition given in Table 4.2. (From Table 4.3 the background concentration of U in the EBPW is 2.1×10^{-8} M, indicated by the dashed line.)

6.7 Se(IV) sorption data

6.7.1 Se kinetics

Table 6.12: Summary of the conditions used in the kinetic measurements of Se on MX-80 bentonite in the porewater composition given in Table 4.2.

Time (days)	S:L ratio (g L ⁻¹)	Total conc. (M)	pH
1; 7; 21; 61	7.4	10 ⁻³ ; 10 ⁻⁴ ; 7 x 10 ⁻⁹	7.6 - 7.7

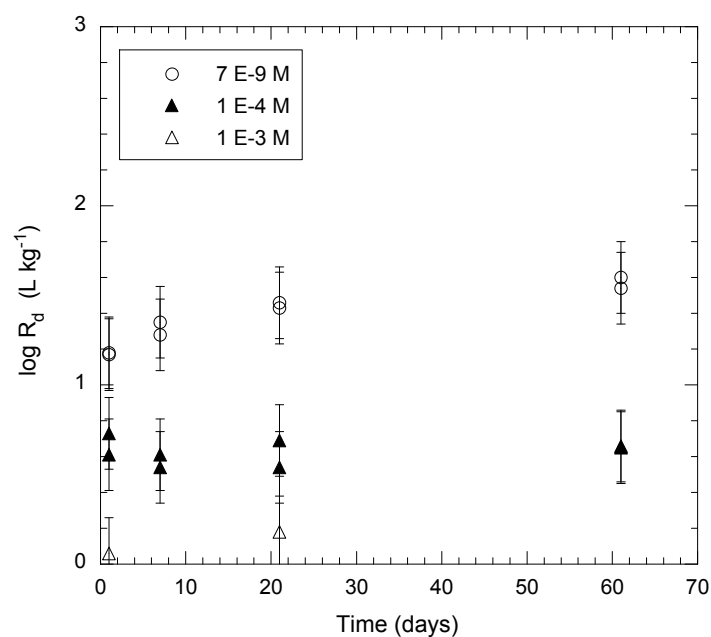


Fig. 6.11: Sorption kinetics of Se uptake on MX-80 in batch experiments.

6.7.2 Se isotherm

Table 6.13: Summary of the conditions used in the isotherm measurements of Se on MX-80 bentonite.

Time (days)	S:L ratio (g L ⁻¹)	Equilibrium conc. range (M)	pH
98	7.4	2.0 x 10 ⁻⁹ to 10 ⁻³	7.6 - 7.7

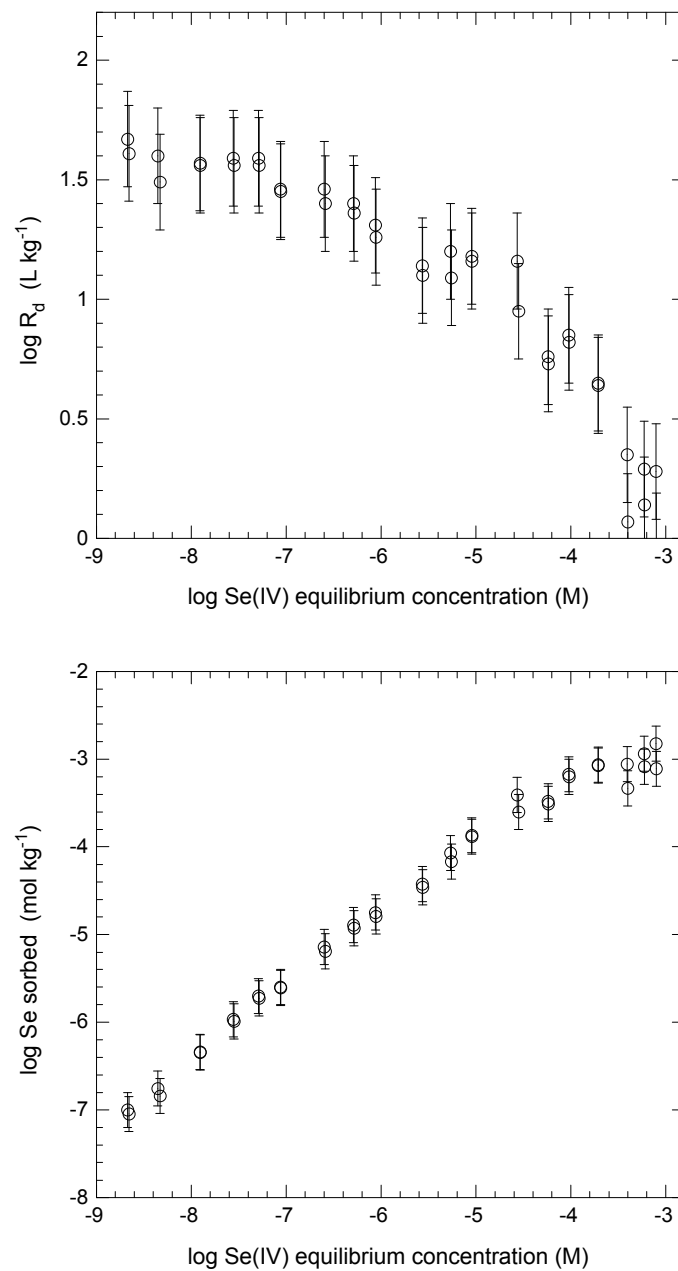


Fig. 6.12: Sorption isotherm of Se on MX-80 measured in batch experiments in the porewater composition given in Table 4.2. (From Table 4.3 the background concentration of Se in the EBPW is $< 1.3 \times 10^{-7}$ M.)

6.8 Cl(-I) and I(-I) sorption measurements

Sorption experiments on Cl(-I) and I(-I) were performed in parallel using essentially the same experimental methodology, described below for Cl⁻. The chloride concentration in the SBPW is high (~0.6 M) and Cl⁻ is usually inert regarding sorption and is not redox sensitive, as is I(-I). Consequently no uptake was expected. The Cl⁻ experiments served as a test to check that the slight uptake of I(-I) on MX-80 subsequently measured (see Figs. 6.13 and 6.14) was not an artefact caused by the measurement methodology.

An 0.5 M NaCl solution was labelled with ³⁶Cl and allowed to equilibrate. 20 ml of the labelled NaCl solution was then added to a known amount of MX-80 bentonite and equilibrated for 3 days with continuous end over end shaking. After this time the suspensions were centrifuged (1 hour at 96000 g_{max}) and the activity of ³⁶Cl was assayed. Experiments were done in triplicate at two different high solid to liquid ratios. The pH in these tests was 7.

The results of these measurements are summarised in Table 6.14. From the analysis 2 parameters can be calculated. The first is the classical solid to liquid distribution ratio assuming that Cl⁻ is accessible to all water present in the bentonite (no anion exclusion). The second parameter which can be calculated is the exclusion volume. This parameter is derived assuming that Cl⁻ is not sorbed on the bentonite, i.e. $R_d = 0$. The results are shown in Table 6.14.

In contrast to I(-I), Figs. 6.13 and 6.14, the calculated R_d values for Cl(-I) were negative in every case. Although this result appears to be anomalous at first sight, the implication is that the whole volume of water in the system is not accessible to Cl⁻, (active ³⁵Cl⁻) i.e. anion exclusion is taking place thus reducing the available volume of water accessible to ³⁵Cl⁻ and hence increasing the measured activity over and above that of the initial solution. The ³⁵Cl⁻ is essentially excluded from the diffuse double layer water and the interlayer water. This of course leads to a negative sorption value.

If the sorption of Cl⁻ is assumed to be zero, a “Cl⁻ excluded volume” can be calculated (De Haan & Bolt 1982). These exclusion volumes are given in Table 6.14.

It is important to note that very high S:L ratios were used in these sorption tests compared to the more usual values of 1 to 10 g L⁻¹. Had the experiments been carried out in the range of the latter S:L ratios then no sorption for I⁻ would have been measured.

Table 6.14: Calculated “ R_d values” and exclusion volumes for Cl⁻.

Sample	S:L ratio (g L ⁻¹)	R_d (L kg ⁻¹)	$V_{\text{exclusion}}$ (ml kg ⁻¹)
1	241.6	-0.30	300.9
2	230.4	-0.30	305.2
3	230.4	-0.32	318.0
4	454.0	-0.28	285.4
5	450.9	-0.29	288.4
6	454.8	-0.28	279.5

6.9 I(-I) sorption data

6.9.1 I(-I) kinetics at 153 g L⁻¹

Table 6.15: Summary of the conditions used in the kinetic measurements of I on MX-80 bentonite.

Time (days)	S:L ratio (g L ⁻¹)	Total conc. (M)	pH
1; 7; 21; 60	153	10 ⁻³ ; 10 ⁻⁵ ; 10 ⁻⁷	7.8

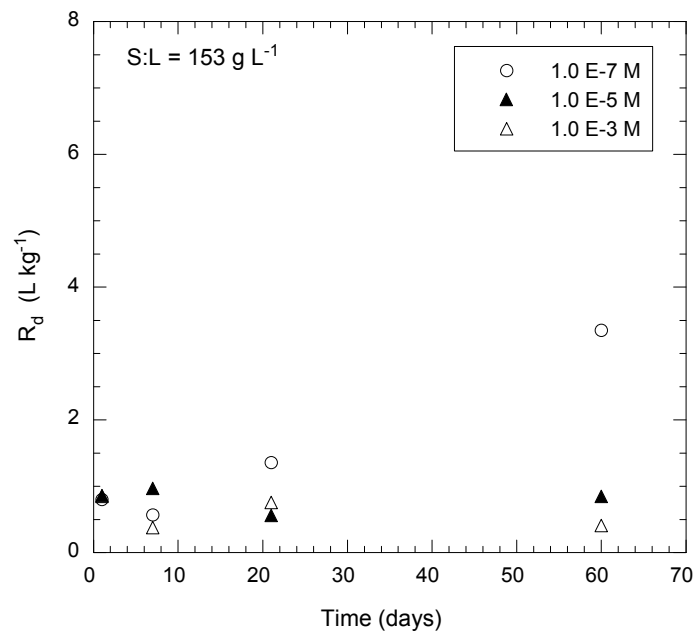


Fig. 6.13: Sorption kinetics of I uptake on MX-80 in batch experiments at 153 g L⁻¹ in the porewater composition given in Table 4.2.

6.9.2 I(-I) kinetics at 303 g L⁻¹

Table 6.16: Summary of the conditions used in the kinetic measurements of I on MX-80 bentonite.

Time (days)	S:L ratio (g L ⁻¹)	Total conc. (M)	pH
1; 7; 21; 60	303	10 ⁻³ ; 10 ⁻⁵ ; 10 ⁻⁷	7.8

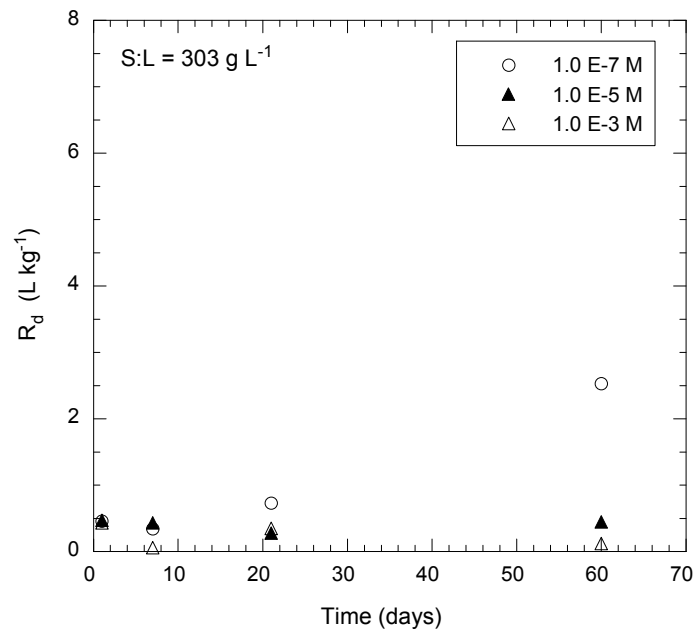


Fig. 6.14: Sorption kinetics of I uptake on MX-80 in batch experiments at 303 g L⁻¹ in the porewater composition given in Table 4.2.

7 Summary

The main aim of this work was to provide a compilation of experimental data on sorption isotherms for key radionuclides on MX-80 bentonite. The primary use of the data obtained from these experiments is in performance assessment studies for radioactive waste disposal in the Swiss programme. However, they also provide basic data sets to test the predictive capacity of mechanistic sorption models e.g. see Bradbury & Baeyens (2005).

In the first part of this work the mineralogy and physico-chemical characteristics of the MX-80 bentonite used in this work are presented: mineralogy, surface areas, sulphate and chloride inventories, CEC, cation occupancies, selectivity coefficients for K-Na, Mg-Na and Ca-Na exchange equilibria, amphoteric edge site capacities and protolysis constants and whole rock analyses (trace element inventories).

A brief discussion on porewater chemistry and the presentation of trace element concentration data for the MX-80 conditioned porewater used in the sorption tests is followed by a description of the preparation/measurement procedures and the sorption methods themselves.

In the second part, the results from kinetic and sorption isotherm batch type experiments for seven elements (Cs, Ni, Eu, Th, U, I and Se¹) are presented for MX-80 bentonite at pH ~7.6. These elements are representative for alkaline, transition metals, trivalent lanthanides/actinides, and tetravalent actinides and hexavalent actinides, respectively. Se and I were chosen because they represent important dose determining radionuclides in performance assessment.

The experiments were carried out under atmospheric conditions. There was no evidence to suggest that there was any influence on the mineralogy of MX-80 or the water chemistry. The valence states of Cs(I), Ni(II), Eu(III) and Th(IV) are stable in air and the same as those expected in the reducing conditions in a radioactive waste repository. However, the results for U(VI) and Se(IV) are not considered to be relevant for reducing conditions where the valence states would be expected to be rather IV and zero/-II respectively. The data for these two elements would be appropriate for a hypothetical oxidising scenario.

Chloride exhibited no measurable sorption under either anoxic or oxic conditions. An anion exclusion volume could be measured from the sorption experiments carried out at high solid:liquid ratios.

A small but definite sorption was measured for I(-I), taking into account the anion exclusion volume measured for chloride. Subsequent measurements under anoxic conditions in an atmosphere controlled N₂ glove box failed to detect any uptake of I by MX-80 bentonite. The reason for the difference in the sorption behaviour of I sorption under oxic and anoxic conditions is not understood.

¹ The chosen elements represent the safety relevant radionuclides considered in Nagra's safety analyses (listed, e.g., in Nagra, 2008) concerning their variety of valence states and migration properties.

Acknowledgements

The contributions of A. Schaible and M. Lauber to the experimental work are gratefully acknowledged. ICP-OES analyses were carried out by S. Köchli. We would like to thank Dr. V. Brendler (FZ Dresden-Rossendorf, Germany) for reviewing the manuscript. Partial financial support was provided by Nagra.

References

- Baeyens, B. & Bradbury, M.H. (1997): A mechanistic description of Ni and Zn sorption on Namontmorillonite. Part I: Titration and sorption measurements. *J. Contam. Hydrol.* 27, 199-222.
- Bolt, G.H. & Van Riemsdijk, W.H. (1987): Surface chemical processes in soils. In: W. Stumm (Editor) *Aquatic Surface Models*. Wiley, New York.
- Bradbury, M.H. & Baeyens, B. (1997): A mechanistic description of Ni and Zn sorption on Namontmorillonite. Part II: Modelling. *J. Contam. Hydrol.* 27, 223-248.
- Bradbury, M.H. & Baeyens, B. (1998a): N₂-BET surface area measurements on crushed and intact minerals and rocks: A proposal for estimating sorption transfer factors. *Nuclear Technology* 122, 250-253.
- Bradbury, M.H. & Baeyens, B. (1998b): A physico-chemical characterisation and geochemical modelling approach for determining porewater chemistries in argillaceous rocks. *Geochim. Cosmochim. Acta* 62, 783-795.
- Bradbury, M.H. & Baeyens, B. (2002): Porewater chemistry in compacted re-saturated MX-80 bentonite: Physico-chemical characterization and geochemical modeling. PSI Bericht Nr. 02-10, Nagra Tech. Rep. NTB 01-08.
- Bradbury, M.H. & Baeyens, B. (2009): Experimental and modelling studies on the pH buffering of MX-80 bentonite porewater. *Appl. Geochem.* doi:10.1016/j.apgeochem. 2008,12.023.
- Bruggenwert, M.G.M. & Kamphorst, A. (1982): Survey of experimental information on cation exchange in soil systems. In *Soil Chemistry B. Physico-chemical Models*. (ed. G.H. Bolt), Vol. 5B, Chap. 5, Elsevier.
- Curti, E. & Wersin, P. (2002): Assessment of porewater chemistry in the bentonite buffer for the Swiss SF/HLW repository. Nagra Tech. Rep. NTB 02-09.
- Gaines, G.I. & Thomas, H.C. (1953): Adsorption studies on clay minerals. II. A formulation of the thermodynamics of exchange adsorption. *J. Chem. Phys.* 21, 714-718.
- Grauer, R. (1986): Bentonite as a backfill material in the high-level waste repository: Chemical aspects. EIR Bericht Nr. 576, Nagra Tech. Rep. NTB 86-12E.
- Grim, R.E. (1953): *Clay mineralogy*. McGraw Hill, New York.
- Karland, O. (2010) Chemical and mineralogical characterization of the bentonite buffer for the acceptance control procedure in a KBS-3 repository. Technical Report SKB TR-10-60.
- Kruse, K. (1992): Die Adsorption von Schwermetallionen an verschiedenen Tonen. Ph.D. Thesis, ETH -Diss. 9737, ETH Zurich, Switzerland.
- Keren, R. & Shainberg, I. (1975): Water vapor isotherms and heat of immersion of Na/Ca-montmorillonite systems. I: Homoionic clay. *Clays Clay Minerals* 23, 193-200.
- Maes, A. & Cremers, A. (1986): High selective ion exchange in clay minerals and zeolites. In *Geochemical Processes at Mineral Surfaces* (eds. J.A. Davis & K.F. Hayes). ACS Symp. Series 323, 254-295.
- Mehra, O.P. & Jackson, M.L. (1960): Iron oxide removal from soils and clays by dithionite-citrate system buffered with sodium bicarbonate. *Clays Clay Minerals* 7, 317-327.
- Müller-Vonmoos, M. & Kahr, G. (1982): Bereitstellung von Bentoniten für Laboruntersuchung. Nagra Tech. Rep. NTB 82-04.
- Müller-Vonmoos, M. & Kahr, G. (1983): Mineralogische Untersuchungen von Wyoming Bentonite MX-80 und Montigel. Nagra Tech. Rep. NTB 83-13.

- Nagra (2008): Vorschlag geologischer Standortgebiete für das SMA- und das HAA-Lager. Begründung der Abfallzuteilung, der Barriersysteme und der Anforderungen an die Geologie. Bericht zur Sicherheit und technischen Machbarkeit. Nagra NTB 08-05.
- Newman, A.C.D. (1987): The interaction of water with clay mineral surfaces. In: Chemistry of Clays and Clay Minerals. (Ed. A.C.D. Newman) Mineralogical Society. Monograph No. 6. Essex, Longman.
- Pearson Jr., F.J. & Berner, U. (1991): Nagra thermochemical data base I. Core data. Nagra Tech. Rep. NTB 91-17.
- Pearson, F.J., Berner, U. & Hummel, W. (1992): Nagra thermo-chemical data base II. Supplemental Data 05/92. Nagra Tech. Rep. NTB 91-18.
- Peigneur, P. (1976): Stability and adsorption affinity of some transition metal-amine complexes in aluminosilicates. Ph.D Thesis, Univ. Leuven, Belgium.
- Pusch, R., Karnland, O. & Hokmark, H. (1990): GMM - A general microstructural model for qualitative and quantitative studies of smectite clays. SKB Technical Report 90-43, Swedish Nuclear Fuel and Waste Management, Stockholm, Sweden.
- Sauzeat, E., Guillaume, D., Villieras, F., Dubessy, J., Francois, M., Pfeiffert, C., Pelletier, M., Ruck, R., Barres, O., Yvon, J. & Cathelineau, M. (2001) Caracterisation Mineralogique, Cristalochimique et Texturale de l'Argile MX-80, ANDRA.
- Sposito, G. & Fletcher, P. (1985): Sodium-calcium-magnesium exchange reactions on a montmorillonitic soil: III Calcium-magnesium exchange selectivity. Soil Sci. Soc. Am. J. 49, 1160-1163.
- Sposito, G., Holtzclaw, K.M., Charlet, L., Jouany, C. & Page, A.L. (1983a): Sodium-calcium and sodium-magnesium exchange on Wyoming bentonite in perchlorate and chloride background ionic media. Soil Sci. Soc. Am. J. 47, 51-56.
- Sposito, G., Holtzclaw, K.M., Jouany, C. & Charlet, L. (1983b): Cation selectivity in sodium-calcium, sodium-magnesium, and calcium-magnesium exchange on Wyoming bentonite at 298 K. Soil Sci. Soc. Am. J. 47, 917-921.
- Tsipursky, S.I. and V.A. Drits, The distribution of octahedral cations in the 2:1 layers of dioctahedral smectites studied by oblique-texture electron diffraction. Clay Minerals, 1984. 19(2): p. 177-193.
- Van Olphen, H. (1963): An introduction to clay colloid chemistry. Interscience Publishers, J. Wiley and Sons, New York.
- Van Olphen, H. and Fripiat, J.J. (1979): Data handbook for clay minerals and other non-metallic minerals. Pergamon Press, Oxford.
- Wanner, H., Wersin, P., & Sierro, N. (1992): Thermodynamic modelling of bentonite-groundwater interaction and implications for near field chemistry in a repository for spent fuel. SKB Technical Report 92-37, Swedish Nuclear Fuel and Waste Management, Stockholm, Sweden.
- Westall, J., Zachary, J.L., & Morel, F. (1976): MINEQL: A computer program for the calculation of chemical equilibrium composition of aqueous systems. Technical Note 18, Dept. of Civil Eng., Massachusetts Institute of Technology, Cambridge, Massachusetts.